RSC Advances

Check for updates

Positive modulators of *N*-methyl-D-aspartate receptor: structure–activity relationship study on steroidal C-17 and C-20 oxime ethers

Santosh Kumar Adla, [a] Barbora Hrčka Krausová,[b] Bohdan Kysilov,[b] Karel Kudláček,[a] Radko Souček,[a] Miloš Budešínský,[a] Jan Voldřich,[ac] Ladislav Vyklický[b] and Eva Kudová [*a]

N-methyl-D-aspartate receptors (NMDARs) are crucial therapeutic targets, modulated by endogenous neurosteroids like pregnenolone sulfate (**PES**). This study investigates a novel structure–activity relationship approach focusing on the steroidal D-ring, employing the bioisosteric replacement of C-17 or C-20 keto groups with oximes and oxime ethers. We synthesized a series of pregn-5-ene and androst-5-ene derivatives (**11–23**) and evaluated their positive allosteric modulator (PAM) activity on recombinant GluN1/GluN2B receptors *via* a patch-clamp technique in HEK293 cells. Our study revealed that pregnenolone-derived C-20 oxime ethers are potent and efficacious PAMs of NMDAR. Several analogues have been demonstrated as more potent than **PES** ($E_{max} = 116\%$; $EC_{50} = 21.7\ \mu M$). Compound **12** (C-20 ethyl oxime ether, C-3 hemiglutarate) displayed the highest efficacy, potentiating NMDAR currents over 6-fold greater than **PES** ($E_{max} = 673 \pm 121\%$; $EC_{50} = 8.7 \pm 1.1\ \mu M$). Compound **17** (C-20 methyl oxime ether analogue) exhibited the highest potency, being over 3.5-fold more potent than **PES** ($E_{max} = 503 \pm 68\%$; $EC_{50} = 6.1 \pm 0.4\ \mu M$). In contrast, some C-17 analogues and derivatives with bulkier C-20 oxime substituents showed complex modulatory behavior. Promisingly, key compounds demonstrated favorable *in vitro* ADME profiles, including high metabolic stability and, for **12**, excellent thermodynamic solubility. These results validate C-20 oxime ether modification of the pregnenolone scaffold as an effective strategy for generating potent NMDAR PAMs with potentially superior efficacy and drug-like properties compared to endogenous modulators.

Introduction

Endogenous neurosteroids such as 20-oxo-5β-pregnan-3α-yl sulfate (pregnanolone sulfate, **PAS**, Fig. 1A) and 20-oxo-pregn-5-en-3β-yl sulfate (pregnenolone sulfate, **PES**, Fig. 1A) are well-established modulators of *N*-methyl-D-aspartate receptors (NMDARs).[1,2] PES acts as a positive allosteric modulator (PAM) of NMDARs, whereas **PAS** functions as a negative allosteric modulator (NAM). NMDARs are heteromeric, Ca^{2+}-permeable ion channels that play a critical role in synaptic plasticity and neurotransmission.[3] Consequently, their activity has been identified as a promising pharmacological target for a range of neurological and psychiatric disorders, including epilepsy and autism,[4–6] post-traumatic stress disorder,[7] depression,[8] pain,[9,10] stroke,[11] and various neurodegenerative diseases.[12]

Mutations in NMDA receptor subunit genes are well-documented in neurodevelopmental and neuropsychiatric disorders.[13–18] Many disease-associated *de novo* variants result in loss-of-function phenotypes with reduced receptor activity and impaired glutamatergic signalling. Consequently, pharmacological strategies to enhance NMDAR function are a promising therapeutic direction.

Beyond these endogenous neurosteroids, numerous synthetic neuroactive steroid analogues have been shown to allosterically modulate NMDARs.[19–24] The mode of action of these compounds is primarily dictated by the structural features of the steroidal skeleton. Specifically, NMDAR inhibition is associated with a bent steroid ring system characterized by 3α-hydroxy-5β-stereochemistry (Fig. 1B). In contrast, potentiation of NMDARs is predominantly linked to a planar skeleton with a 3β-hydroxy-Δ5,6-ene configuration (featuring a double bond in the B-ring, Fig. 1B), a structural motif that has been extensively studied.[20,25]

As part of our ongoing research on neurosteroid modulators of NMDARs, we have conducted several structure–activity relationship (SAR) studies to elucidate the pharmacophore

aInstitute of Organic Chemistry and Biochemistry of the Czech Academy of Sciences, Flemingovo Namesti 2, Prague 6 – Dejvice, 16610, Czech Republic. E-mail: kudova@uochb.cas.cz

bInstitute of Physiology of the Czech Academy of Sciences, Videnska 1083, Prague 4, 14220, Czech Republic

cUniversity of Chemistry and Technology, Technicka 5, Prague 6, 166 28, Czech Republic
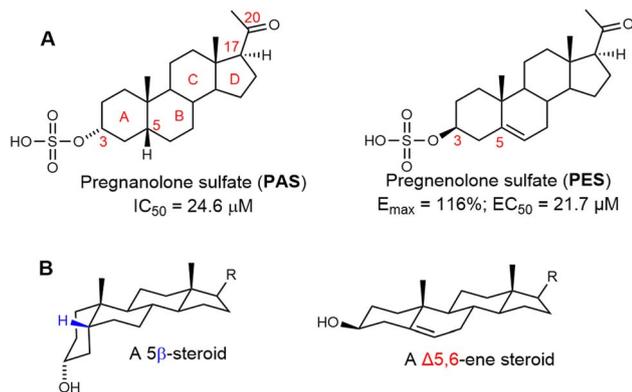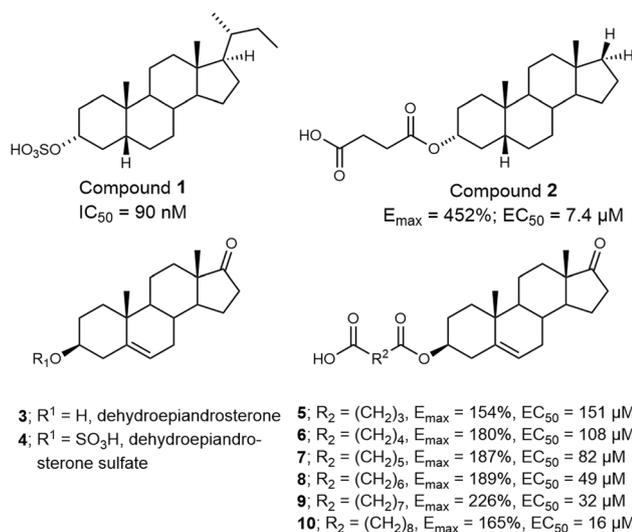
Fig. 1 Steroidal positive and negative allosteric modulators of NMDA receptors. (A) Structures of endogenous neurosteroids pregnanolone sulfate (PAS) and pregnenolone sulfate (PES) with ring letters and skeleton numbering relevant for this publication. (B) Simplified visualization of a bent molecule of 5β- and planar Δ5,6-ene steroids.
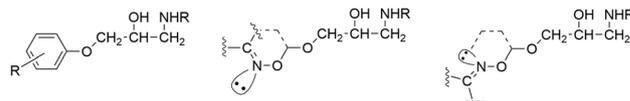
requirements for steroidal PAMs and NAMs. Our findings indicate that NMDAR modulatory activity is highly dependent on the presence of a charged substituent, such as a sulfate moiety.[26] Specifically, replacing the sulfate group with uncharged substituents abolishes NAM activity, whereas substitution with dicarboxylic acid esters generally preserves activity.[20,26]

Further, we have explored the impact of non-lipophilic substituents at the C-17 position of the steroidal D-ring on *in vitro* activity.[19,20] Our studies demonstrated that the allosteric modulatory effect—either positive or negative—correlates with the lipophilicity of the compound. For example, compound **1** (Fig. 2), featuring an isobutyl chain at C-17, inhibited currents of GluN1/GluN2B receptors with an IC_{50} of 90 nM.[19] Similarly, removing the C-17 substituent in compound **2** resulted in potentiation of GluN1/GluN2B receptor responses, with an E_{max} of 452% and an EC_{50} of 7.4 μM.[20]

Interestingly, neither our SAR studies nor those by other researchers have extensively investigated polar modifications of the steroidal D-ring. Based on literature data, substitution of C-

3; R^1 = H, dehydroepiandrosterone
4; R^1 = SO_3H, dehydroepiandrosterone sulfate

5; R_2 = $(CH_2)_3$, E_{max} = 154%, EC_{50} = 151 μM
6; R_2 = $(CH_2)_4$, E_{max} = 180%, EC_{50} = 108 μM
7; R_2 = $(CH_2)_5$, E_{max} = 187%, EC_{50} = 82 μM
8; R_2 = $(CH_2)_6$, E_{max} = 189%, EC_{50} = 49 μM
9; R_2 = $(CH_2)_7$, E_{max} = 226%, EC_{50} = 32 μM
10; R_2 = $(CH_2)_8$, E_{max} = 165%, EC_{50} = 16 μM

Fig. 2 Structures of PAMs and NAMs of NMDARs.

Fig. 3 Proposed electronic distribution of aliphatic oxime ethers and their aromatic analogue from Macchia et al.[30]

17 with a ketone is expected to yield inactive compounds, as observed for dehydroepiandrosterone and dehydroepiandrosterone sulfate.[27] Contrary to this expectation, our 2018 study[20] revealed that compounds **5–10** function as PAMs with moderate efficacy. While compounds within this structural series exhibited similar maximal efficacy (E_{max} ranging from 154% to 226%), their potency varied significantly, with EC_{50} values between 16 and 151 μM.

The replacement of the keto group with a suitable surrogate, or (bio)isostere, can represent an effective strategy for SAR studies targeting novel analogues, as such modification should preserve at least similar biological activities of the parent compound.[28,29] For our study, the replacement of C-17 and C-20-ketone groups with a lipophilic-like surrogate was proposed.

The modification of a ketone into an aliphatic oxime ether was selected as the most promising candidate for further evaluation. Interestingly, according to the literature, the electronic distribution of aliphatic oxime ether derivatives can mimic that of aromatic groups (Fig. 3). A seminal study from 1985 (ref. 30) reported that a series of methyleneaminoxy methyl derivatives ($C=NOCH_2$) exhibited *in vitro* activity on β-adrenoceptors comparable to their aromatic analogues. The bioisosteric potential of the oxime ether moiety as a replacement for aryl groups has been extensively reviewed.[28]

Oximes are widely studied nitrogen- and oxygen-containing structural motifs with diverse biological and pharmacological applications,[31] including indications related to central nervous system (CNS) disorders, as they are capable of permeating the blood–brain barrier.[32,33] Notably, oximes have been extensively investigated as antidotes for organophosphate poisoning, with pyridine-2-aldoxime (pralidoxime) being the only FDA-approved treatment for this condition to date.[31] Additionally, golexanolone, a novel neurosteroid-based γ-aminobutyric acid receptor (GABA$_A$R) antagonist, is currently in development for the treatment of cognitive impairment associated with hepatic encephalopathy.[34–36]

In this study, we report the synthesis of C-17 and C-20 oximes and oxime ethers (compounds **11–23**) and evaluate their biological activity on recombinant GluN1/GluN2B receptors expressed in human embryonic kidney (HEK293) cells. Additionally, key pharmacokinetic properties were assessed *in vitro*, including stability in rat liver microsomes and parallel artificial membrane permeability (PAMPA). For the most potent compound, **12**, further evaluations were conducted to determine plasma stability, stability in primary rat hepatocytes, and thermodynamic solubility.

Results and discussion

Chemistry

The proof-of-concept of our hypothesis of biologically active steroidal oximes and oxime ethers was evaluated on two basic
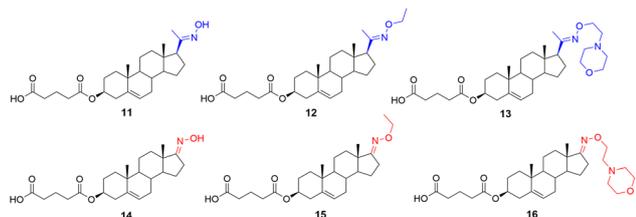
Fig. 4 Proof-of-concept molecules 11–16.

steroidal skeletons. Compounds 11–13 were prepared from 3β-hydroxy-pregn-5-en-20-one (pregnenolone), and compounds 14–16 (Fig. 4) were prepared from 3β-hydroxy-androst-5-en-17-one (dehydroepiandrosterone, DHEA, 3).

A steroidal skeleton with a C-3 hemiglutarate ester moiety was selected based on our previous SAR study on pregn-5-en and androst-5-ene derivatives.[20] Oximation at positions C-6 or C-7 is well documented in the literature, as hydroxyimino steroids represent a distinct class of antineoplastic agents.[37,38] Following a review of synthetic strategies for steroidal ketoximes and oxime ethers, we evaluated two methods for introducing the hydroxyimino group at C-20 of pregnenolone (Scheme 1): (i) reaction with hydroxylamine hydrochloride in aqueous ethanol in the presence of sodium acetate (NaOAc)[39] and (ii) reaction with hydroxylamine hydrochloride in ethanolic pyridine or pyridine with triethylamine.[40–42] Both approaches provided comparable isolated yields exceeding 90% (synthesis of compound 24). The treatment of O-alkyl hydroxylamine hydrochloride with sodium acetate was subsequently applied to the synthesis of all target compounds.

Next, we explored two synthetic sequences for the introduction of the hydroxyimino and hemiester moieties (Scheme 1) in the synthesis of compound 12. This approach was designed to generate a parent compound that could be further modified at C-3 with ester linkers of varying lengths or novel oxime ethers. Compound 12 was synthesized via oximation of the C-20 ketone of pregnenolone using hydroxylamine hydrochloride in aqueous ethanol with NaOAc, yielding compound 24 (98%). This was followed by esterification of the C-3 hydroxyl group with glutaric acid in the presence of EDCI, DMAP, and DIPEA, affording compound 12 in 89% yield.

Alternatively, pregnenolone was first esterified at C-3 with glutaric anhydride and DMAP in pyridine, yielding compound
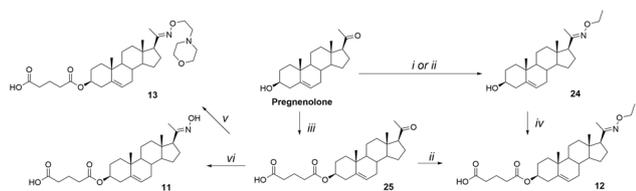
Scheme 1 Synthesis of compounds 11, 12, and 13. Reagents and conditions: (i) NH$_2$OEt·HCl, NaOAc, EtOH/H$_2$O, 95 °C; (ii) NH$_2$-OEt·HCl, pyridine, Et$_3$N, EtOH/H$_2$O, 95 °C; (iii) glutaric anhydride, DMAP, pyridine, 105 °C; (iv) glutaric acid, EDCI, DMAP, DIPEA, DCM, rt; (v) 4-[2-(aminooxy)ethyl]morpholine, NaOAc, EtOH/H$_2$O, 95 °C; (vi) NH$_2$OH·HCl, NaOAc, EtOH/H$_2$O, 95 °C.
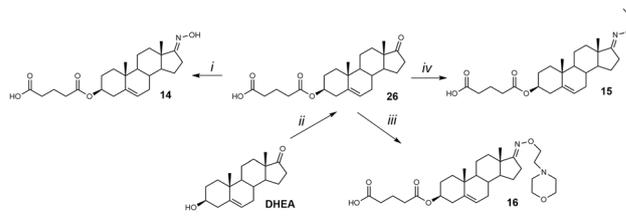
Scheme 2 Synthesis of compounds 14, 15, and 16. Reagents and conditions: (i) NH$_2$OH·HCl, NaOAc, EtOH/H$_2$O, 95 °C; (ii) glutaric anhydride, DMAP, pyridine, 105 °C; (iii) 4-[2-(aminooxy)ethyl]morpholine, NaOAc, EtOH/H$_2$O, 95 °C; (iv) NH$_2$O-ethyl HCl, NaOAc, EtOH/H$_2$O, 95 °C.

25 (57%). Subsequent treatment of compound 25 with O-ethyl-hydroxylamine hydrochloride (NH$_2$OEt·HCl/NaOAc) resulted in compound 12 (64%). Additionally, compound 25 was treated with NH$_2$OEt·HCl/NaOAc to yield compound 11 (82%), while compound 13 was prepared using freshly synthesized 4-[2-(aminooxy)ethyl]morpholine in 62% yield.[43]

Since both synthetic approaches yielded comparable isolated yields, we prioritized the sequence involving hemiester formation followed by oxime synthesis for the preparation of compounds 15 and 16 (Scheme 2). This decision was further supported by our previous experience with low-yielding esterification steps in the synthesis of various hemiesters.[20]

Accordingly, DHEA (3) was first esterified with a hemiglutarate moiety at C-3, affording compound 26 in 50% yield. Subsequent oximation with NH$_2$OEt·HCl/NaOAc yielded compound 14 in 85% yield. Finally, compounds 15 and 16 were synthesized by treating DHEA with NH$_2$OEt·HCl and 4-[2-(aminooxy)ethyl]morpholine/NaOAc, respectively, yielding compound 15 (52%) and compound 16 (77%).

The biological activity of compounds 11–16 (Fig. 4) was evaluated on recombinant GluN1/GluN2B receptors expressed in HEK293 cells. Our results demonstrated that pregnenolone analogues (11–13) exhibited greater activity than their DHEA-derived counterparts. The reference compound – pregnenolone sulfate – produced a potentiation with a maximal response (E_{max}) near baseline (116%), and a potency of EC$_{50}$ = 21.7 μM. Several compounds of series 11–16 displayed enhanced efficacy compared to PES. Pregnenolone derivatives 11 and 12 both substantially increased the current amplitude, with 12 showing the greatest potentiation (673 ± 121%) and EC$_{50}$ value of 8.7 μM. DHEA derivative 15 also displayed marked potentiation (441 ± 76%), statistically significant, but with lower potency (EC$_{50}$ = 22.7 μM), aligning more closely with PES. Consequently, further compound development focused exclusively on modifying the pregnenolone skeleton. Based on these findings, we designed a series of pregnenolone oxime ethers 17–21 (Fig. 5).

Compounds 17–21 were synthesized by reacting pregnenolone 3-hemiglutarate (25) with the corresponding oxime reagent in the presence of NaOAc (Scheme 3). Compound 17 was obtained using O-methyl hydroxylamine hydrochloride (NH$_2$-OCH$_3$·HCl) in 73% yield, compound 18 with O-propyl hydroxylamine hydrochloride (NH$_2$OCH$_2$CH$_2$CH$_3$·HCl) in 55% yield, and compound 19 with O-isopropyl hydroxylamine
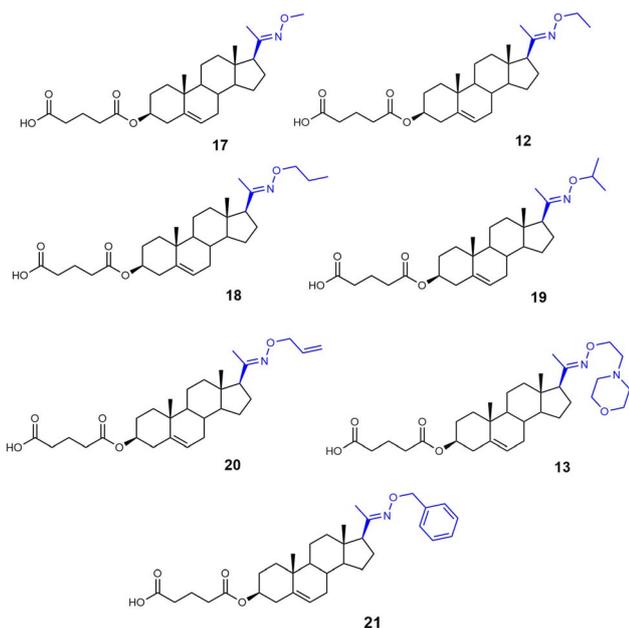
Fig. 5 A series of oxime ethers modifications of pregnenolone 3-hemiglutarate 12, 13, and 17–21.

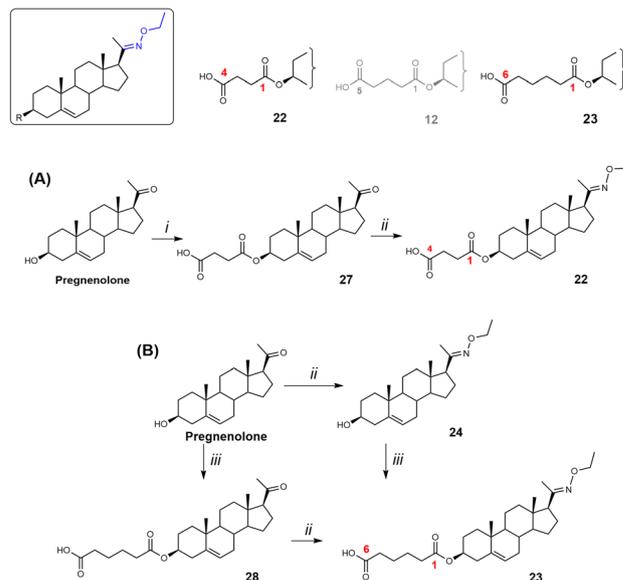Scheme 4 Synthesis of compounds 22 and 23. Reagents and conditions: (i) succinic acid, EDCI, DMAP, DIPEA, DCM, rt; (ii) NH2-ethyl HCl, NaOAc, EtOH/H2O, 95 °C; (iii) adipic acid, EDCI, DMAP, DIPEA, DCM, rt.

hydrochloride (NH$_2$OCH(CH$_3$)$_2$·HCl) in 49% yield. Treatment with O-allyl hydroxylamine hydrochloride (NH$_2$OCH$_2$CH= CH$_2$·HCl) afforded compound 20 in 63% yield, while reaction with O-benzyl hydroxylamine hydrochloride (NH$_2$OCH$_2$C$_6$H$_5$-·HCl) produced compound 21 in 89% yield.

The biological activity of compounds 17–21 (Fig. 5) was evaluated on recombinant GluN1/GluN2B receptors expressed in HEK293 cells. Our results showed that the structural modifications in compounds 17–21 did not enhance the PAM effect compared to compound 12, yet compound 17 showed the greatest potentiation (503 ± 85%) and EC$_{50}$ value of 6.1 μM. Consequently, we synthesized analogues of compound 12 with hemiester linkers of varying lengths (Scheme 4).

The C-3 hemisuccinate (compound 22) was prepared via a two-step synthesis (Scheme 4). First, the C-3 hydroxy group of pregnenolone was esterified with succinic acid using EDCI, DMAP, and DIPEA, affording compound 27 in 57% yield. Subsequent oximation with NH$_2$OEt·HCl/NaOAc yielded

compound 22 in 71% yield. The C-3 hemiadipate (compound 23) was synthesized analogously. Pregnenolone was esterified with adipic acid in the presence of EDCI, DMAP, and DIPEA, giving compound 28 in a yield of 35%. Similarly, an attempt to esterify compound 24 yielded only 13% of compound 23, with 40% of the starting material recovered. These low esterification yields are consistent with our previously published results.[20]

Finally, the biological activity of compounds 22 and 23 was evaluated on recombinant GluN1/GluN2B receptors expressed in HEK293 cells. Our results showed that the structural modifications in compounds 22 and 23 did not enhance the PAM effect compared to compound 12.

To unambiguously assign the structure of compound 12, which could exist in interconvertible E- and Z-stereoisomerism (Fig. 6), we have performed the structural assignment of the proton and carbon signals by combining 1D-^{1}H and ^{13}C spectra with homonuclear 2D-H,H-COSY and 2D-H,H-ROESY, and heteronuclear 2D-H,C-HSQC and 2D-H,C-HMBC spectra on a Bruker 600 AVANCE III instrument (^{1}H at 600.13 MHz and ^{13}C at 150.9 MHz) with a 5 mm cryoprobe in CDCl$_3$ solutions at 25 °C. Experimental evidence for configuration on the C(20) = N double bond based on NOE contacts of CH$_2$ or CH$_3$ protons was not successful, likely due to the long distance of these protons to either C(21)H$_3$ in the E-isomer or C(16)H and C(17)H$_2$ in the Z-isomer. The geometry optimization on the model of both

Scheme 3 Synthesis of compounds 17–21. Reagents and conditions: (i) For 17: NH$_2$O-methyl HCl, NaOAc, EtOH/H$_2$O, 95 °C; (ii) For 18: NH$_2$O-propyl HCl, NaOAc, EtOH/H$_2$O, 95 °C; (iii) For 19: NH$_2$O-iso-propyl HCl, NaOAc, EtOH/H$_2$O, 95 °C; (iv) For 20: NH$_2$O-allyl HCl, NaOAc, EtOH/H$_2$O, 95 °C; (v) For 21: NH$_2$O-benzyl HCl, NaOAc, EtOH/H$_2$O, 95 °C.
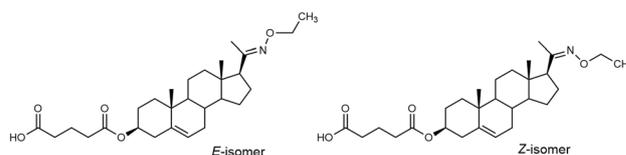
Fig. 6 E- and Z-isomers of compound 12.

Table 1 The ^{13}C and ^{1}H NMR data of compound **12**

Position	Type	Carbon	Proton
1	–CH$_2$–	36.96	1.865; 1.145
2	–CH$_2$–	27.74	1.855; 1.585
3	>CH–O	74.22	4.62 m
4	–CH$_2$–	28.08	2.31 (2H)
5	>C=	139.60	N/A
6	=CH–	122.50	5.375 m
7	–CH$_2$–	31.77	2.00; 1.57
8	>CH–	31.99	1.465
9	>CH–	50.04	0.995
10	>C<	36.62	N/A
11	–CH$_2$–	20.97	1.57; 1.445
12	–CH$_2$–	38.56	1.88; 1.30
13	>C<	43.70	N/A
14	>CH–	56.12	1.11
15	–CH$_2$–	24.27	1.675; 1.205
16	–CH$_2$–	23.16	2.16; 1.67
17	>CH–	56.64	2.22
18	–CH$_3$	13.19	0.64
19	–CH$_3$	19.32	1.02
20	>C=N	157.40	N/A
21	–CH$_3$	15.78	1.82
N–O–CH$_2$–CH$_3$			
	O–CH$_2$–	68.72	4.085
	–CH$_3$	14.74	1.24
3-O–CO–CH$_2$–CH$_2$–CH$_2$–COOH			
	C=O	172.27	N/A
	–CH$_2$–	33.50	2.37 (2H)
	–CH$_2$–	19.87	1.95 (2H)
	–CH$_2$–	32.86	2.43 (2H)
	COOH	178.27	N/A

isomers suggested a slightly lower potential energy for the *E*-isomer; however, this difference is insufficient to serve as definitive evidence of configuration. The ^{1}H and ^{13}C NMR data are in Table 1.

Effects of compounds 11–23 on responses of GluN1/GluN2B receptors in HEK293 cells to glutamate

To investigate the effect of compounds **11–23** on the activity of NMDARs, electrophysiological measurements were performed on HEK293 cells that were co-transfected with cDNAs containing genes encoding for the rat GluN1-1a and GluN2B subunits. The degree of modulation (E; potentiation/inhibition) for the newly synthesized compounds was determined using the following formula:

$$E = \frac{(I_e - I_a)}{I_e} \times 100$$

where I_e is the value of the current amplitude during glutamate and compound coapplication, and I_a is the current amplitude value for glutamate application. The degree of potentiation (%) was determined for five compound doses, differing 100-fold in their concentration range, in individual cells, and data were fitted to the following equation:

$$E = E_{max} \bigg/ \left(1 + \left(\frac{EC_{50}}{[\text{compound}]} \right)^h \right)$$

where E_{max} is the maximal value of potentiation induced by a saturating concentration of the compound, EC_{50} is the concentration of the compound that produces half-maximal potentiation of the agonist-evoked current, [compound] is the compound concentration, and h is the apparent Hill coefficient. The results are presented as mean ± standard error of the mean (SEM), with n equal to the number of independent measurements. One-way analysis of variance (ANOVA) was used for multiple comparisons (unless otherwise stated, a value of $P \leq 0.05$ was used for the determination of significance).

The overview of the concentration-dependent effects of compounds **11–23** on responses of GluN1/GluN2B receptors in HEK293 cells to glutamate is summarized in Table 2.

We have evaluated the relationship between oxime derivatives **11–23** and their modulatory effect on recombinant GluN1/GluN2B receptors. Due to the disuse-dependent effect of neurosteroid-based PAMs at NMDARs[20,44] GluN1/GluN2B receptors were activated by 1 μM glutamate, a concentration corresponding to the EC_{50} value for this agonist, to reveal the maximal modulatory effect of the tested compounds during coapplication. We focused on GluN2B-containing receptors, as we previously demonstrated that pregnane-based steroids with PAM activity can compensate for NMDAR hypofunction caused by the *de novo* missense variant L825V in the GluN2B subunit.[45]

Our data shows that 8 out of 13 newly synthesized compounds had PAM effect at GluN1/GluN2B receptors, with increased efficacy (in case of compounds **12, 15, 17,** and **23** significantly) and/or potency (in case of compounds **11, 17,** and **22** significantly) as compared to endogenous sulfate analogue **PES**. Three compounds – **14, 18,** and **19** – were not identified as

Table 2 Parameters from the concentration-response analysis of the effect of compounds **11–23** on glutamate-induced currents of GluN1/GluN2B receptors expressed in HEK293 cells[a]

No.	E_{max} ± SEM (%)	EC_{50} ± SEM (μM)	h ± SEM	n
PES (ref. 20)	116 ± 10	21.7 ± 1.6	1.5 ± 0.1	10
11	270 ± 35	7.9 ± 2.1*	1.5 ± 0.1	5
12	673 ± 121***	8.7 ± 1.1	1.7 ± 0.3	7
13	111 ± 11	34.7 ± 4.2	2.8 ± 0.2**	5
14	N/A#	N/A#	N/A#	7
15	441 ± 76**	22.7 ± 3.1	1.5 ± 0.1	7
16	44 ± 5	63.5 ± 6.4	1.7 ± 0.1	4
17	503 ± 85**	6.1 ± 0.7*	1.6 ± 0.1	4
18	NAM (7 ± 2%) at 3 μM		N/A	4
	PAM (75 ± 21% and 108 ± 17%) at 10 and 30 μM			
19	NAM (27 ± 5%) at 3 μM		N/A	5
	PAM (81 ± 20% and 169 ± 55%) at 10 and 30 μM			
20	317 ± 43	12.6 ± 2.9	2.0 ± 0.2	5
21	403 ± 56	11.3 ± 2.0	1.7 ± 0.3	4
22	340 ± 22	7.0 ± 1.1*	1.3 ± 0.1	7
23	451 ± 79*	7.5 ± 1.1	1.7 ± 0.1	5
One-way ANOVA	$P < 0.001$	$P < 0.001$	$P = 0.013$	

[a] PAM, positive allosteric modulator; NAM, negative allosteric modulator; NA, not analysed; #Compound 14 had no effect at the concentration range of 3–100 μM and was toxic for the HEK293 cells, which precluded the analysis. One-way ANOVA on ranks with Kruskal–Wallis post hoc analysis *versus* PES; *$P > 0.05$; **$P > 0.01$; ***$P > 0.001$.

PAMs of NMDARs. In contrast, compounds **14**, **18**, and **19** exhibited a more complex concentration-dependent pharmacological profile, acting as PAMs at certain concentrations while displaying antagonistic effects at others. This behavior is less common but has been observed for some compounds. For example, several ligand-gated ion channels are modulated by ivermectin, including the glutamate-gated chloride channel, GABA$_A$R, glycine receptor, α7-nicotinic acetylcholine receptor, and P2X4 purinergic receptor.[46] Ivermectin enhances the activity of these channels in a concentration-dependent manner; at lower concentrations, it potentiates agonist-induced responses, whereas at higher concentrations, it can activate the channels independently of the agonist. Concentration dependence has also been shown for neurosteroids. For example, the U-shaped dose–response curve on the normalized peak amplitude of I_{GABA} has been shown in the Purkinje cells of the cerebellum. In particular, allopregnanolone, pregnanolone, and **PAS** enhanced I_{GABA} between 10 and 5000 nM. This effect was reversed at higher concentrations from 10 to 100 μM.[47,48]

As mentioned above, within the structural family of this study, the majority of compounds exhibited PAM effect on NMDARs with more than 16-fold difference in the E_{max} values (44% for the least efficacious compound **16** compared to 673% for the most efficacious compound **12**), with EC$_{50}$ values varying from 6.1 μM for the most potent compound **17** to 63.5 μM for the least potent compound **16**.

First, we compared the biological activity of C-17 *versus* C-20 oxime derivatives using recombinant GluN1/GluN2B receptors expressed in HEK293 cells. Our findings revealed that pregnenolone-based oximation displayed overall high PAM-activity. Compound **12** emerged as the most efficacious compound in the series. In contrast, the C-17 hydroxy oxime analogue of DHEA (**14**) lost its PAM-activity, and the morpholine-substituted analogue **16** proved to be the least effective derivative in the study. Next, we explored the replacement of the pregnenolone C-20 ketone group with various oxime moieties. As oximation represents an effective strategy for SAR studies, a wide range of reagents is readily available for this purpose. We selected and prepared a series of aliphatic and branched alk(en)yl oximes (**17–20**), along with benzyl (**21**) analogue, and morpholine analogues (**13**), in which the substituent is linked to the pregnenolone scaffold *via* the oxime functionality. Interestingly, within the series of alk(en)yl oximes (**12**, **13**, **17–20**), the methyl (**17**) and ethyl (**12**) oximes emerged as the most efficacious compounds, exhibiting E_{max} values of 673% and 503%, respectively. The corresponding EC$_{50}$ values were 6.1 μM for compound **17** and 8.7 μM for compound **12**. In contrast, the propyl (**18**) and isopropyl (**19**) analogues displayed a complex, concentration-dependent activity profile. Both compounds potentiated agonist-induced responses at 3 μM, but at higher concentrations (10–30 μM), their effects shifted toward inhibition. The presence of a double bond within the oxime moiety in compounds **20** (allyl) and **21** (benzyl) resulted in comparable efficacy, with E_{max} values of 317% and 403%, respectively. The corresponding EC$_{50}$ values were 12.6 μM for compound **20** and 11.3 μM for compound **21**. Our SAR study revealed that modifications of the oxime moiety did not result
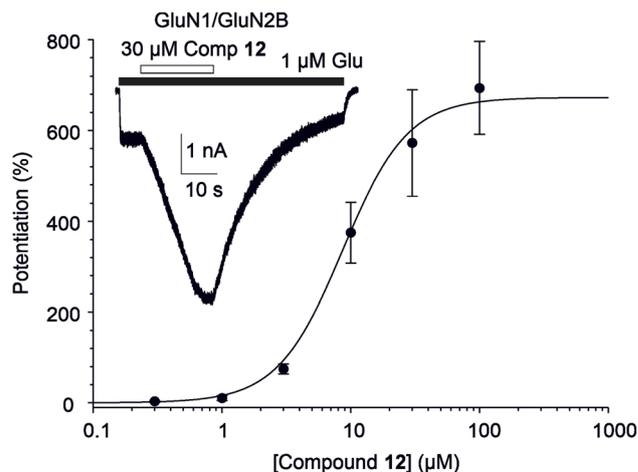

Fig. 7 The effect of compound **12** on GluN1/GluN2B receptors. The graph shows the concentration-response curve for the effect of compound **12** at GluN1/GluN2B receptors. Data points are averaged values of potentiation at given concentration (0.3–100 μM) from 7 independent measurements; error bars represent SEM. The degree of potentiation of glutamate-induced responses recorded in the presence of compound **12** was determined in individual cells, and data were fitted to the logistic equation (obtained parameters for compound **12** are indicated in Table 2). The inset shows an example of a trace recorded from a HEK293 cell expressing recombinant GluN1/GluN2B receptors. Compound **12** (30 μM) was applied simultaneously with 1 μM glutamate and 30 μM glycine (the duration of compound **12** and glutamate application is indicated by open and filled bars, respectively).

in improved efficacy compared to compound **12**. Consequently, we turned our attention to the C-3 hemiester moiety. Compounds **22** (hemisuccinate) and **23** (hemiadipate) were evaluated for their ability to modulate NMDARs. Both compounds demonstrated comparable efficacy, with E_{max} values of 340% and 451%, respectively. The corresponding EC$_{50}$ values were 7.0 μM for compound **22** and 7.5 μM for compound **23**. Compound **12** was identified as the most efficacious compound of the study (Fig. 7).

In Vitro ADME profiling – metabolic stability, permeability assessment, and solubility

The results of *in vitro* ADME profiling are summarized in Table 3. First, the metabolic stability of compounds **11–23** was assessed using rat liver microsomes. Briefly, each compound was incubated with microsomes for 60 min, followed by extraction and analysis *via* LC-MS. Verapamil was used as a control due to its well-characterized metabolic elimination and relatively short half-life.[49] Remarkably, nearly all tested compounds demonstrated high metabolic stability, with half-lives exceeding 60 min. Notably, compounds **12**, **19–21**, and **23** exhibited exceptional stability, showing no detectable metabolism after 60 min of incubation.

Second, the permeability of compounds **11–23** was evaluated using the parallel artificial membrane permeability assay (PAMPA), a widely accepted method for predicting brain penetration.[50–53] Atenolol and verapamil served as reference

Table 3 ADME Assessment of compounds **11–23**

Steroid	Stability in rat microsomes		PAMPA permeability		Solubility	Stability in rat plasma (% remaining)		Stability in primary rat hepatocytes	
	$t_{1/2}$ (min)	Cl_{int} (μlmin^{-1}mg)	P_e (cm s^{-1})	Retention (%)	PBS, pH 7.4 (μM)	8 h	24 h	$t_{1/2}$ (min)	Cl_{int} (μl min^{-1} mg^{-1})
11	58.6 ± 18.7	23.6	1.55×10^{-4}	87	—	69.9 ± 6.0	58.1 ± 8.1		
12	$>>60^a$	—	3.89×10^{-6}	97	361 ± 41	85.6 ± 1.0	59.6 ± 0.7	72.4	19.1
13	>60	—	n.d.	95	—	—	—	—	—
14	>60	—	2.63×10^{-5}	17	—	61.1 ± 1.6	56.3 ± 2.5	—	—
15	>60	—	1.82×10^{-3}	80	—	82.1 ± 7.5	69.9 ± 5.0	—	—
16	>60	—	6.76×10^{-5}	17	—	82.1 ± 5.8	73.1 ± 7.8	—	—
17	>60	—	5.50×10^{-6}	95	—	—	—	—	—
18	>60	—	n.d.	100	—	—	—	—	—
19	$>>60^a$	—	n.d.	99	—	—	—	—	—
20	$>>60^a$	—	7.24×10^{-6}	99	—	—	—	—	—
21	$>>60^a$	—	1.82×10^{-6}	95	—			—	—
22	52.6 ± 3.7	26.3	1.58×10^{-6}	96	22 ± 1	94.7 ± 5.7	76.7 ± 4.7	—	—
23	$>>60$	—	n.d	100	21 ± 1	85.7 ± 4.6	56.3 ± 3.0	—	—
Verapamil	43.9 ± 1.2	31.5	3.72×10^{-4}	33	—	—	—	—	—
Atenolol	—	—	1.07×10^{-7}	31	—	—	—	—	—
Imipramine	—	—	—	—	—	—	—	20.6	67.3

^{a} The compound exhibits a half-life significantly exceeding 60 min, with no detectable decrease in intensity over time. Where referred, results are presented as mean $\pm$ SEM; n.d., not defined.

compounds for low and high permeability, respectively.[54] Permeability was quantified using permeability coefficients (P_e) and mass retention, the latter representing the proportion of compound retained in the membrane. Compounds **11** and **15** exhibited permeability comparable to or greater than that of verapamil; compounds **14** and **16** exhibited moderate permeability. Among the series, compound **15** was identified as the most permeable. High mass retention values (>80%) were observed for most compounds, indicating strong membrane interaction, except compounds **14** and **16**, which showed high permeability but low mass retention (17%). These findings suggest that structural modifications of the DHEA scaffold can yield derivatives with favourable permeability profiles. However, it is important to note that compounds **14** and **16** were inactive *in vitro* despite their favourable permeability characteristics.

Next, we evaluated the stability in rat plasma and thermodynamic solubility in PBS (pH 7.4) for proof-of-concept compounds (compounds **11**, **12**, **14–16**), as well as for the most potent compound at NMDAR-induced currents (**12**) and its analogues (**22** and **23**). All compounds showed comparable stability within 8 and 24 h. Compound **12** also demonstrated moderate metabolic stability in rat hepatocytes. Overall, the results for rat plasma stability and hepatic clearance were consistent with those observed in rat microsomes. Notably, the tested compounds exhibited unexpected stability of the hemiester bond after 8 h, suggesting that these compounds could potentially be suitable for preliminary *in vivo* studies.

Finally, to test our hypothesis that introducing an oxime ether moiety could enhance the drug-like properties of our compounds, we compared the rat plasma stability of compounds **12**, **22**, and **23** with their corresponding 20-ketone analogues.[20] The results, summarized in Table 4, show that the

oxime ether moiety indeed improved the plasma stability of these compounds.

We evaluated compounds **11–23** in a series of *in vitro* assays designed to assess key parameters relevant to their bioavailability profiles. Our results indicate that substitution of the steroidal scaffold with an oxime or oxime ether moiety yielded compounds with unexpectedly high stability in both rat microsomes and rat plasma, despite the presence of a hemiester group at the C-3 position. This is particularly notable, as the hemiester moiety is generally considered susceptible to rapid

Table 4 Comparison of the solubility and rat plasma stability of oxime ethers **12**, **22**, and **23** with that of their corresponding 20-ketone analogues

Steroid	Solubility in PBS 7.4 (μM)	Stability in rat plasma (% remaining)	
		8 h	24 h
22	22 ± 1	95 ± 6	77 ± 5
12	361 ± 41	86 ± 1	60 ± 1
23	21 ± 1	86 ± 5	56 ± 3
20-Oxo-PE-hSuc	277 ± 1	69 ± 1	50 ± 2
20-Oxo-PE-hGlu	86 ± 1	44 ± 3	21 ± 1
20-Oxo-PE-hAdi	20 ± 2	11 ± 0	2 ± 0
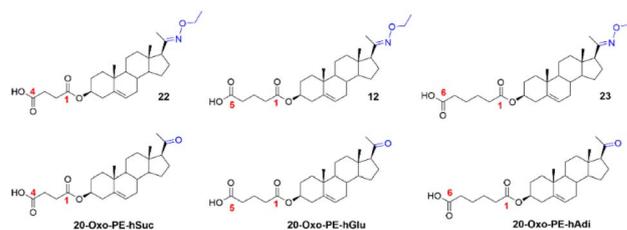
hydrolysis by carboxylesterases, as reported in the literature.[55] Furthermore, our experiments demonstrated that certain lipophilic steroidal derivative (compound **12**) can demonstrate excellent thermodynamic solubility (>350 μM) atypical for steroidal compounds.

Our previous SAR study on pregn-5-ene dicarboxylic acid esters (hOxa, hMal, hSuc, hGlu, hAdi, hPim, hSub) for their modulation of recombinant GluN1/GluN2B receptors demonstrated their positive modulatory effect with EC_{50} varying from 8.5 to 48.6 μM and E_{max} varying from 93% to 191%.[20] The chemical basis for the superior efficacy of pregnenolone-derived C-20 oxime ethers compared with the parent 20-keto steroids and with PES can be rationalized by several structural features. First, the introduction of the C-20 oxime ether converts the polar carbonyl into a more extended C=N–O–R motif, which increases local lipophilicity and provides an additional hydrogen bond acceptor. Within the series **12**, **13**, **17–21**, small O-alkyl substituents (methyl **17**, ethyl **12**) yield very high E_{max} values (673% for **12** and 503% for **17**) while maintaining low micromolar EC_{50} (8.7 and 6.1 μM, respectively), whereas bulkier or more rigid substituents (propyl **18**, isopropyl **19**, allyl **20**, benzyl **21**) reduce efficacy or introduce biphasic PAM/NAM profiles. This trend suggests that the oxime ether substituent might occupy a defined pocket within the GluN1/GluN2B allosteric site, where steric bulkiness or conformational rigidity leads to suboptimal binding modes or alternative interactions, such as accessibility of the allosteric binding site between helices that promote inhibition at higher concentrations.

Second, the C-3 hemiester functions as a tunable polar moiety that modulates overall amphiphilicity without disrupting the planar 5-ene steroid core known to favor NMDAR potentiation. Direct comparison of the results from our previous study on pregn-5-ene-20-one compounds with those of the present study indicates that hemisuccinate and hemiglutarate substitution preserves both efficacy and potency. This suggests that the negatively charged terminal carboxylate primarily contributes to anchoring at the membrane or protein surface rather than engaging a highly specific molecular interaction. Consequently, the superior profile of **12**, **22**, and **23** therefore appears to arise from an optimal combination of C-20 oxime ether lipophilicity and C-3 linker length, which together enhance receptor engagement while maintaining excellent solubility and metabolic stability.

Finally, comparison of pregnenolone- and DHEA-based analogues highlights the importance of the D-ring oxidation pattern and side-chain geometry. Pregnenolone-derived oxime ethers showed higher PAM efficacy than the corresponding DHEA C-17 oximes (**14–16**), with **14** completely losing PAM activity and **16** being the least efficacious compound. This observation supports a model in which the C-20 substituent projects more favorably into the allosteric binding region than C-17.

Experimental

General

Dichloromethane was refluxed over phosphorous pentoxide under an inert atmosphere for 30 min, followed by distillation.

The chemicals and reagents were purchased from commercial suppliers and used without further purification. Melting points were determined with a micromelting point apparatus (Hund/ Wetzlar, Germany) and are uncorrected. For elemental analysis, the PE 2400 Series II CHNS/O Analyzer (PerkinElmer, MA, USA) was used, with microbalance MX5 (Mettler Toledo, Switzerland). For measurement of optical rotation, AUTOPOL IV (Rudolph Research Analytical, NJ, USA) was used; all samples were measured at 20 °C, at a given concentration in a given solvent at 589 nm. Analytical samples were dried over phosphorus pentoxide at 50 °C/100 Pa. The HRMS spectra were performed with LTQ Orbitrap XL (Thermo Fischer Scientific, MA, USA) in ESI mode. Thin-layer chromatography (TLC) was performed on silica gel (Merck, 60 μm). Proton and carbon NMR spectra were measured in a Bruker AVANCE-400 FT NMR spectrometer (400 MHz, 101 MHz) in CDCl₃, with tetramethylsilane as the internal standard. Chemical shifts are given in ppm (δ scale). Coupling constants (J) and widths of multiplets (W) are given in Hz. IR spectra were recorded on a Nicolet 6700 spectrometer (wavenumbers in cm-1). MS High-resolution MS spectra were performed with a Q-Tof microspectrometer (Waters). LC-MS was measured by two methods. Method A: using LC-MS system (C4 column Phenomenex 250 mm length, 2 mm width, Jupiter 300–5 C4, TSP quaternary pump P4000, TSP autosampler AS3000) equipped with UV/VIS detector (UV6000LP, UV/VIS setup wavelength range 190–700 nm, bandwidth 1 nm, step 1 nm, and scan rate 1 Hz) and ion-trap mass spectrometer Advantage (positive ion mode with m/z range from 220 to 1000 Da). Solvent A was 98% water/2% acetonitrile, and B was 95% acetonitrile/3% isopropanol/2% water with 5 mM ammonium formate. Gradient setup: 0-25-30-30.1-45 min 50-100-100-50-50% solvent B and flow rate 150 μL min⁻¹. Method B: Analysis was carried out on the UHPLC-MS system Nexera LC-40 (Shimadzu, Japan) equipped with ELS and MS detectors. Ions were detected: MS, positive DUIS (ESI/APCI) ion mode, with m/z range from 250 to 1000 Da, interface temp. 350 °C, desolvation line temp. 250 °C, nebulizing gas flow 1.5 L min⁻¹, heat block temp. 400 °C, drying gas 15 L min⁻¹. ELSD, desolvation temp. 60 °C, gain 10. Solvent A was water/methanol/ formic acid (950 : 50 : 1), and solvent B was acetonitrile. Analysis was performed in an isocratic mode with 80% of solvent B, and a flow rate of 0.5 mL min⁻¹, column: Shim-pack Scepter, C8-120, 1.9 μm, 100 × 2.1 mm (Shimadzu). The sample was prepared by dissolving the material (1 mg) in methanol (1 mL, LC-MS grade) and then sonicated for 5 min. Injection volume varied from 0.1 to 0.4 μL. The percentage purity of compounds was calculated from the ratio of peaks in the ELSD chromatogram.

The purity of the final compounds was assessed by a combination of NMR and based on LC-HR-MS analysis or elemental analysis, and the results showed they were greater than 95%.

Nitrosamine risk assessment

The synthetic route used in the synthesis employs hydroxylamine hydrochloride and O-alkylhydroxylamine hydrochlorides and tertiary amine bases (DIPEA, triethylamine, pyridine). None of the steroidal oximes or oxime ethers contain (**11–23**) a stable

secondary or tertiary amine; the nitrogen is present exclusively as an oxime/oxime ether functionality (C=N–O–R), which is not considered a typical precursor for *N*-nitrosamine formation under standard pharmaceutical processing conditions. Hydroxylamine salts and *O*-alkylhydroxylamines are consumed during the reaction and the residual amount is removed by aqueous work-up and the following chromatography. Considering the intended use of these compounds *in vitro* and prospective *in vivo* studies, nitrosamines derived from DIPEA and triethylamine are regarded as process-related impurities that were effectively removed during work-up and solvent evaporation. Overall, these factors support a very low risk of nitrosamine presence in the final products.

Impurity profiling and toxicological considerations

The impurity profile of each final compound was assessed using a combination of ^{1}H/^{13}C NMR, LC-HRMS or ELSD-based HPLC, and all target oximes and oxime ethers were obtained with a purity ≥95%. Given that these compounds are at a non-clinical, exploratory research stage and used solely *in vitro* at low micromolar concentrations, toxicological qualification of trace impurities was not pursued. The ADME experiments were conducted with material meeting these purity criteria, therefore the observed pharmacological and ADME properties can be attributed to the parent compounds rather than to impurities.

General procedure: synthesis of oxime ethers with *O*-alkyl hydroxylamine hydrochloride and sodium acetate

A mixture of *O*-alkyl hydroxylamine hydrochloride (0.58 mmol), sodium acetate (NaOAc) (1.05 mmol), and steroid (0.23 mmol) was dissolved in an aqueous ethanol solution (EtOH/H$_2$O, 10 : 1, 20 mL). The reaction mixture was heated at 95 °C, and the progress of the reaction was monitored periodically by TLC. If the conversion was low after 24 hours, additional *O*-alkyl hydroxylamine hydrochloride and NaOAc were added, and the mixture was heated at 95 °C for a further 24 hours. After cooling to room temperature, the reaction mixture was poured into water (50 mL) and extracted with dichloromethane (3 × 50 mL). The combined organic layers were washed with brine (50 mL), dried over Na$_2$SO$_4$, and concentrated under reduced pressure. The crude product was purified by column chromatography.

Synthesis of compounds 11–28

20-Oxo-pregn-5-en-3β-yl 3-hemiglutarate 20-oxime (**11**). Compound **11** was prepared according to the general procedure. Starting from compound **25** (150 mg, 0.35 mmol), compound **11** (129 mg, 82%) was obtained by column chromatography (5–10% methanol in dichloromethane). Recrystallization from acetone/heptane afforded LC-MS purity of 99%. Mp 185–186 °C. [α]$_D$ −13.6 (*c* 0.2, CHCl$_3$). ^{1}H NMR (400 MHz, CDCl$_3$): δ 0.62 (s, 3H, H-18), 1.01 (s, 3H, H-19), 1.94 (s, 3H, H-21), 1.96–1.99 (m, 2H, HOOC–CH$_2$–CH$_2$–CH$_2$), 2.38 (t, *J* = 7.1 Hz, 2H, HOOC–CH$_2$–CH$_2$–CH$_2$), 2.43 (t, *J* = 7.0 Hz, 2H, HOOC–CH$_2$–CH$_2$–CH$_2$), 4.60–4.71 (m, 1H, H-3), 5.37 (d, *J* = 5.8 Hz, 1H, H-5). ^{13}C NMR (101 MHz, CDCl$_3$): δ 178.21 (COOH), 172.50 (ester CO), 159.49 (C=N–OH), 139.73 (C-5), 122.57 (C-6), 73.79 (C-3), 56.74, 56.02, 50.02, 44.37, 38.49, 38.32, 37.08, 36.81, 33.38, 32.72,

32.22, 31.90, 27.85, 24.43, 23.44, 21.08, 20.30, 19.56, 16.00, 13.38. IR spectrum (CHCl$_3$): 3591, 3274 (oxime OH), 3510, 3097 (COOH), 1723 (C=O), 1655 (C=C). MS (negative ESI): *m/z* 445.3 (35%, M), 444.3 (100%, M − H). HR-MS (negative ESI) *m/z*: For C$_{26}$H$_{38}$O$_5$N [M − H] calcd, 444.2755; found, 444.2753.

20-Oxo-pregn-5-en-3β-yl hemiglutarate O-ethyloxime (**12**). Compound **12** was prepared according to the general procedure. Starting from compound **25** (100 mg, 0.23 mmol), compound **12** (98 mg, 89%) was obtained as an oily compound by column chromatography (10–20% acetone in dichloromethane) with an LC-MS purity of 99%. [α]$_D$ −13.7 (*c* 0.3, CHCl$_3$). ^{1}H NMR (400 MHz, CDCl$_3$): δ 0.64 (s, 3H, H-18), 1.02 (s, 3H, H-19), 1.24 (t, 3H, *J* = 7.0 Hz, O–CH$_2$–CH$_3$), 1.82 (s, 3H, H-21), 1.93–1.98 (m, 2H, HOOC–CH$_2$–CH$_2$–CH$_2$), 2.37 (t, *J* = 7.3 Hz, 2H, HOOC–CH$_2$–CH$_2$–CH$_2$), 2.43 (t, *J* = 7.3 Hz, 2H, HOOC–CH$_2$–CH$_2$–CH$_2$), 4.03–4.12 (m, 2H, O–CH$_2$–CH$_3$), 4.59–4.65 (m, 1H, H-3), 5.37 (d, *J* = 5.0 Hz, 1H, H-6). ^{13}C NMR (101 MHz, CDCl$_3$): δ 178.27 (COOH), 172.27 (ester CO), 157.40 (C=N), 139.60, 122.50 (C-6), 74.22 (C-3), 68.72 (O–CH$_2$–CH$_3$), 56.64, 56.12, 50.04, 43.70, 36.96, 38.56, 36.62, 33.50, 32.86, 31.99, 31.77, 28.08, 27.74, 24.27, 23.16, 20.97, 19.87, 19.32 (C-19), 15.78 (C-21), 14.74 (O–CH$_2$–CH$_3$), 13.19 (C-18). IR spectrum (CHCl$_3$): 3517, 3098 (COOH), 2970, 2945 (CH$_3$), 2676 (OH), 1723, 1714 (C=O), 1666 (C=C), 1626 (C=N). MS (ESI): *m/z* 496.3 (20%, M + Na), 474.3 (100%, M + H). HR-MS (ESI) *m/z*: For C$_{28}$H$_{44}$O$_5$N [M − H] calcd, 472.3068; found, 472.3060.

20-Oxo-pregn-5-en-3β-yl hemiglutarate O-(3-morpholinoethyl) oxime (**13**). Compound **13** was prepared according to the general procedure. Starting from compound **25** (200 mg, 0.46 mmol), compound **13** (162 mg, 62%) was obtained as an oily compound by column chromatography (10–20% acetone in dichloromethane) with an LC-MS purity of 99%. [α]$_D$ −19.6 (*c* 0.15, CHCl$_3$). ^{1}H NMR (400 MHz, CDCl$_3$): δ 0.62 (s, 3H, H-18), 1.02 (s, 3H, H-19), 1.80 (s, 3H, H-21), 1.91–1.96 (m, 2H, HOOC–CH$_2$–CH$_2$–CH$_2$), 2.30–2.34 (m, 2H, HOOC–CH$_2$–CH$_2$–CH$_2$), 2.36–2.38 (m, 2H, HOOC–CH$_2$–CH$_2$–CH$_2$), 2.64–2.69 (m, 4H, N–(CH$_2$–CH$_2$)$_2$–O), 2.75–2.79 (m, 2H, O–CH$_2$–CH$_2$–N), 3.73–3.79 (m, 4H, N–(CH$_2$–CH$_2$)$_2$–O), 4.23 (t, *J* = 5.6 Hz, 2H, O–CH$_2$–CH$_2$-morpholine), 4.58–4.66 (m, 1H, H-3), 5.37 (d, *J* = 5.9 Hz, 1H, H-6). ^{13}C NMR (101 MHz, CDCl$_3$): δ 178.31 (COOH), 172.61 (ester CO), 158.01 (C=N–O), 139.80 (C-5), 122.60 (C-6), 74.04 (C-3), 70.35 (O–CH$_2$–CH$_2$–N), 66.39 (2 × C, N–(CH$_2$–CH$_2$)$_2$–O), 57.28 (2 × C, N–(CH$_2$–CH$_2$)$_2$–O), 56.86, 56.31, 53.59, 50.20, 43.81, 38.84, 38.26, 37.16, 36.78, 33.90, 32.18, 31.93, 27.93, 24.39, 23.23, 21.96, 21.17, 20.44, 19.49, 16.21, 13.40. IR spectrum (CHCl$_3$): 3513, 3115, (COOH), 1722 (C=O), 1660 (C=C), 1467, 1455, 1397, 1190, 1138, 967 (morpholine). MS (negative ESI): *m/z* 558.5 (36%, M), 557.5 (100%, M − H). HR-MS (negative ESI) *m/z*: For C$_{32}$H$_{49}$O$_6$N$_2$ [M − H] calcd, 557.3596; found, 557.3594.

17-Oxo-androst-5-en-3β-yl 3-hemiglutarate 17-oxime (**14**). Compound **14** was prepared according to the general procedure. Starting from compound **26** (150 mg, 0.37 mmol), compound **14** (132 mg, 85%) was obtained by column chromatography (5–12.5% methanol in dichloromethane). Recrystallization from acetone/heptane afforded LC-MS purity of 99%. Mp 210–212 °C. [α]$_D$ −49.0 (*c* 0.2, CHCl$_3$). ^{1}H NMR (400 MHz, CDCl$_3$): δ 0.93 (s, 3H, H-18), 1.04 (s, 3H, H-19), 1.91–2.01 (m, 2H,

COOH–CH$_2$–CH$_2$–CH$_2$), 2.35–2.40 (m, 2H, HOOC–CH$_2$–CH$_2$–CH$_2$), 2.39–2.44 (m, 2H, COOH–CH$_2$–CH$_2$–CH$_2$), 4.55–4.68 (m, 1H, H-3), 5.39 (d, J = 4.0 Hz, 1H, H-6). ^{13}C NMR (101 MHz, CDCl$_3$): δ 177.90 (COOH), 172.48 (ester CO), 171.59 (C=N–OH), 139.96 (C-5), 122.15 (C-6), 73.93 (C-3), 54.14, 50.23, 44.17, 38.20, 37.06, 36.84, 33.85, 33.75, 33.12, 31.42, 31.35, 27.89, 25.65, 23.37, 20.63, 20.28, 19.48, 17.03. IR spectrum (CHCl$_3$): 3586, 3296 (oxime OH), 3513, 3122 (COOH), 1723 (C=O), 1682 (C=C). MS (negative ESI): m/z 417.3 (29%, M), 416.3 (100%, M − H). HR-MS (negative ESI) m/z: For C$_{24}$H$_{34}$O$_5$N [M − H] calcd, 416.2442; found, 416.2441.

17-Oxo-androst-5-en-3β-yl hemiglutarate O-ethyloxime (15). Compound **15** was prepared according to the general procedure. Starting from compound **26** (150 mg, 0.37 mmol), compound **15** (152 mg, 92%) was obtained by column chromatography (CH$_2$Cl$_2$/acetone/acetic acid (10 : 1 : 0 to 1 : 1 : 0.1)). Recrystallization from acetone/heptane afforded material with an LC-MS purity of 99%. Mp 73–75 °C. [α]$_D$ −37.7 (c 0.2, CHCl$_3$). ^{1}H NMR (400 MHz, CDCl$_3$): δ 0.91 (s, 3H, H-18), 1.03 (s, 3H, H-19), 1.23 (t, J = 7.0 Hz, 3H, O–CH$_2$–CH$_3$), 1.74–1.87 (m, 2H, HOOC–CH$_2$–CH$_2$–CH$_2$), 1.89–2.09 (m, 2H, HOOC–CH$_2$–CH$_2$–CH$_2$), 2.38–2.52 (m, 2H, HOOC–CH$_2$–CH$_2$–CH$_2$), 4.04–4.08 (m, 2H, O–CH$_2$–CH$_3$), 4.56–4.64 (m, 1H, H-3), 5.37 (d, J = 4.1 Hz, 1H, H-6). ^{13}C NMR (101 MHz, CDCl$_3$): δ 179.15 (COOH), 172.90 (ester CO), 170.15 (C=N–O), 140.02 (C-5), 122.25 (C-6), 73.99 (C-3), 68.91 (O–CH$_2$–CH$_3$), 54.26, 50.37, 43.81, 43.81, 38.23, 37.09, 36.86, 34.22, 32.03, 31.54, 31.42, 27.87, 25.90, 23.47, 20.71, 19.49, 17.18, 14.83, 14.25. IR spectrum (CHCl$_3$): 3516, 3088 (COOH), 2970, 2950 (CH$_3$), 2873, 2861 (CH$_2$), 2650 (OH), 1722, 1713 (C=O), 1670 (C=C), 1655 (C=N–O), 1050, 1043 (O–Et). MS (negative ESI): m/z 444.3 (100%, M − H). HR-MS (negative ESI) m/z: For C$_{26}$H$_{38}$O$_5$N [M − H] calcd, 444.2755; found, 444.2752.

17-Oxo-androst-5-en-3β-yl hemiglutarate O-(3-morpholino-propyl)oxime (16). Compound **16** was prepared according to the general procedure. Starting from **26** (200 mg, 0.49 mmol), compound **16** (202 mg, 77%) – a mixture of E and Z-isomers was obtained as an oily compound by column chromatography (5–12.5% methanol in dichloromethane) with an LC-MS purity of 99%. ^{1}H NMR (400 MHz, CDCl$_3$): δ 0.93 (s, 3H, H-18), 1.06 (s, 3H, H-19), 2.34–2.40 (m, 6H, HOOC–CH$_2$–CH$_2$–CH$_2$), 2.64–2.75 (m, 4H, N–(CH$_2$–CH$_2$)$_2$–O), 2.82 (t, J = 5.6 Hz, 2H, O–CH$_2$–CH$_2$–N), 3.77–3.82 (m, 4H, N–(CH$_2$–CH$_2$)$_2$–O), 4.13–4.30 (m, 2H, O–CH$_2$–CH$_2$–N), 4.58–4.68 (m, 1H, H-3), 5.40 (d, J = 5.0 Hz, 1H, H-6). ^{13}C NMR (101 MHz, CDCl$_3$): δ (mixture of isomers, m = minor), peak for COOH is not visible, 172.67 (ester CO), 170.99 (C=N–O-), 140.00 (C-5), 122.19 (C-6), 73.94 (C-3), 70.27 (O–CH$_2$–CH$_2$–N), 66.38 (m), 66.26 (2C, N–(CH$_2$–CH$_2$)$_2$–O), 57.16 (2C, N–(CH$_2$–CH$_2$)$_2$–O), 57.04 (m), 55.31 (m), 54.25, 53.56 (m), 53.51, 50.32, 50.05 (m), 46.06 (m), 43.97, 38.24, 37.09, 37.02 (m), 36.86, 36.81 (m), 34.16, 33.90, 33.73 (m), 31.50, 31.40, 30.99 (m), 29.84 (m), 29.40 (m), 29.27, 27.88, 26.17, 24.06 (m), 23.44, 22.83 (m), 20.88 (m), 20.68, 20.49, 19.49 (m), 19.41, 17.20, 14.26 (m), 14.01. IR spectrum (CHCl$_3$): 3515, 3115 (COOH), 1723 (C=O), 1668 (C=C), 1467, 1455, 1189, 1143, 1027, 970, 610 (morpholine), 1234, 1116 (ester C–O). MS (negative ESI): m/z 530.4 (38%, M),

529.4 (100%, M − H). HR-MS (negative ESI) m/z: For C$_{30}$H$_{45}$O$_6$N$_2$ [M − H] calcd, 529.3283; found, 529.3282.

20-Oxo-pregn-5-en-3β-yl hemiglutarate O-methyloxime (17). Compound **17** was prepared according to general procedure. Starting from compound **25** (130 mg, 0.30 mmol), compound **17** (101 mg, 73%) was obtained as an amorphous compound by column chromatography (dichloromethane/acetone/acetic acid, 4 : 1 : 0 to 0 : 1 : 0.1). Recrystallization from acetone/heptane afforded an LC-MS purity of 99%. Mp 138–140 °C. [α]$_D$ −26.8 (c 0.17, CHCl$_3$). ^{1}H NMR (400 MHz, CDCl$_3$): δ 0.64 (s, 3H, H-18), 1.02 (s, 3H, H-19), 1.81 (s, 3H, H-21), 2.29–2.34 (m, 2H, HOOC–CH$_2$–CH$_2$–CH$_2$), 2.37 (t, J = 7.3 Hz, 2H, HOOC–CH$_2$–CH$_2$–CH$_2$), 2.43 (t, J = 5.0 Hz, 2H, HOOC–CH$_2$–CH$_2$–CH$_2$), 3.83 (s, 3H, O–CH$_3$), 4.58–4.65 (m, 1H, H-3), 5.38 (d, J = 5.0 Hz, 1H, H-6). ^{13}C NMR (101 MHz, CDCl$_3$): δ 178.24 (COOH), 172.46 (ester CO) 157.69 (C=N–O), 139.78 (C-5), 122.66 (C-6), 74.18 (C-3), 61.33 (O–CH$_3$), 56.76, 56.30, 50.21, 43.78, 38.77, 38.24, 37.14, 36.78, 33.69, 33.06, 32.15, 31.93, 27.91, 24.41, 23.23, 21.14, 20.09, 19.48, 15.77, 13.30. IR spectrum (CHCl$_3$): 3516, 3090 (COOH), 2967, 2943 (CH$_3$), 2670 (OH), 1726, 1713 (C=O), 1670 (C=C), 1626 (C=N). MS (negative ESI): m/z 458.3 (100%, M − H). HR-MS (negative ESI) m/z: For C$_{27}$H$_{40}$O$_5$N [M − H] calcd, 458.2912; found, 458.2909.

20-Oxo-pregn-5-en-3β-yl hemiglutarate O-propyloxime (18). Compound **18** was prepared according to the general procedure. Starting from compound **25** (130 mg, 0.30 mmol), compound **22** (81 mg, 55%) was obtained as an amorphous compound by column chromatography (5–10% methanol in dichloromethane). Recrystallization from acetone/heptane afforded LC-MS purity of 99%. Mp 70.5–72 °C. [α]$_D$ −27.7 (c 0.2, CHCl$_3$). ^{1}H NMR (400 MHz, CDCl$_3$): δ 0.63 (s, 3H, H-18), 0.92 (t, J = 7.4 Hz, 3H O–CH$_2$–CH$_2$–CH$_3$), 1.02 (s, 3H, H-19), 1.82 (s, 3H, H-21), 1.91–1.97 (m, 2H, HOOC–CH$_2$–CH$_2$–CH$_2$), 2.37 (t, J = 7.3 Hz, 2H, HOOC–CH$_2$–CH$_2$–CH$_2$), 2.43 (t, J = 7.3 Hz, 2H, HOOC–CH$_2$–CH$_2$–CH$_2$), 3.98 (td, J = 6.7, 2.1 Hz, 2H, O–CH$_2$–CH$_2$), 4.62 (dt, J = 11.6, 6.8 Hz, 1H, H-3), 5.38 (d, J = 5.1 Hz, 1H, H-5). ^{13}C NMR (101 MHz, CDCl$_3$): δ 178.10 (COOH), 172.45 (ester CO), 157.20 (C=N–O), 139.78 (C-5), 122.68 (C-6), 75.00 (O–CH$_2$–CH$_2$), 74.19 (C-3), 56.88, 56.30, 50.23, 43.80, 38.78, 38.25, 37.14, 36.79, 33.69, 33.03, 32.17, 31.95, 27.92, 24.43, 23.28, 22.69, 21.15, 20.10, 19.48, 15.89, 13.34, 10.56 (O–CH$_2$–CH$_2$–CH$_3$). IR spectrum (CHCl$_3$): 3516, 3088 (COOH), 2672 (OH), 1727, 1713 (C=O), 1671 (C=C), 1626 (C=N). MS (negative ESI): m/z 487.3 (28%, M), 486.3 (100%, M − H). HR-MS (negative ESI) m/z: For C$_{29}$H$_{44}$O$_5$N [M − H] calcd, 486.3225; found, 486.3218.

20-Oxo-pregn-5-en-3β-yl hemiglutarate O-isopropyloxime (19). Compound **19** was prepared according to general procedure. Starting from compound **25** (130 mg, 0.30 mmol), compound **22** (72 mg, 49%) was obtained as an amorphous compound by column chromatography (5–10% methanol in dichloromethane). Recrystallization from acetone/heptane afforded LC-MS purity of 98%. Mp 114–116 °C. [α]$_D$ +12 (c 0.2, CHCl$_3$). ^{1}H NMR (400 MHz, CDCl$_3$): δ 0.64 (s, 3H, H-18), 1.02 (s, 3H, H-19), 1.21 (d, J = 6.2, 1.0 Hz, 6H, O–CH(CH$_3$)$_2$), 1.80 (s, 3H, H-21), 1.93–2.02 (m, 2H, HOOC–CH$_2$–CH$_2$–CH$_2$), 2.37 (t, J = 7.3 Hz, 2H, HOOC–CH$_2$–CH$_2$–CH$_2$), 2.43 (t, J = 7.3 Hz, 2H, HOOC–CH$_2$–CH$_2$–CH$_2$), 4.28 (hept, J = 6.2 Hz, 1H, O–

CH(CH$_3$)$_2$), 4.56–4.68 (m, 1H, H-3), 5.38 (d, J = 5.0 Hz, 1H, H-6). ^{13}C NMR (101 MHz, CDCl$_3$): δ 177.94 (COOH), 172.45 (ester CO), 156.58 (C=N–O), 139.78 (C-5), 122.70 (C-6), 74.42 (O–CH(CH$_3$)$_2$), 74.20 (C-3), 57.01, 56.32, 50.25, 43.78, 38.79, 38.25, 37.15, 36.79, 33.69, 32.99, 32.18, 31.96, 27.92, 24.43, 23.36, 21.97, 21.85, 21.16, 20.09, 19.48, 16.03, 13.35. IR spectrum (CHCl$_3$): 3517, 3089 (COOH), 2672 (OH), 1754, 1725, 1713 (C=O), 1671 (C=C), 1629 (C=N). MS (negative ESI): m/z 486.3 (100%, M − H). HR-MS (negative ESI) m/z: For C$_{29}$H$_{44}$O$_5$N [M − H] calcd, 486.3225; found, 486.3219.

20-Oxo-pregn-5-en-3β-yl hemiglutarate O-(2-propenyl)oxime (20). Compound **20** was prepared according to the general procedure. Starting from compound **25** (100 mg, 0.23 mmol), compound **20** (71 mg, 63%) was obtained as an amorphous compound by column chromatography (10–35% acetone in dichloromethane). Recrystallization from acetone/heptane afforded LC-MS purity of 99%. Mp 91–93 °C. [α]$_D$ −21.8 (c 0.2, CHCl$_3$). ^{1}H NMR (400 MHz, CDCl$_3$): δ 0.64 (s, 3H, H-18), 1.02 (s, 3H, H-19), 1.84 (s, 3H, H-21), 1.91–1.99 (m, 2H, HOOC–CH$_2$–CH$_2$–CH$_2$), 2.37 (t, J = 7.3 Hz, 2H, HOOC–CH$_2$–CH$_2$–CH$_2$), 2.43 (t, J = 7.3 Hz, 2H, HOOC–CH$_2$–CH$_2$–CH$_2$), 4.54 (dt, J = 5.6, 1.5 Hz, 2H, N–O–CH$_2$), 4.57–4.68 (m, 1H, H-3), 5.16 (dt, J = 10.5, 1.5 Hz, 1H, CH=CH$_2$), 5.26 (dq, J = 17.3, 1.7 Hz, 1H, CH=CH$_2$), 5.37 (dd, J = 4.5, 2.8 Hz, 1H, H-6), 5.99 (ddt, J = 17.3, 10.7, 5.5 Hz, 1H, CH=H$_2$). ^{13}C NMR (101 MHz, CDCl$_3$): δ 178.49 (COOH), 172.43 (ester CO), 157.88 (C=N–O), 139.77 (C-5), 135.06 (O–CH$_2$–CH=CH$_2$), 122.66 (C-6), 116.79 (O–CH$_2$–CH=CH$_2$), 74.35 (N–O–CH$_2$–CH=CH$_2$), 74.19 (C-3), 56.83, 56.29, 50.21, 43.80, 38.76, 38.24, 37.13, 36.78, 33.67, 33.04, 32.15, 31.93, 27.91, 24.41, 23.26, 21.14, 20.05, 19.47, 16.00, 13.35. IR spectrum (CHCl$_3$): 3516, 3083 (COOH), 3011 (=CH), 1724, 1713 (C=O), 1671 (C=C), 1647 (vinyl C=C), 1624 (C=N). MS (ESI): m/z 486.3 (100%, M + H). HR-MS (ESI) m/z: For C$_{29}$H$_{44}$O$_5$N [M + H] calcd, 486.3214; found, 486.3214.

20-Oxo-pregn-5-en-3β-yl hemiglutarate O-(phenylmethyl)oxime (21). Compound **21** was prepared according to the general procedure. Starting from compound **25** (100 mg, 0.23 mmol), compound **21** (111 mg, 90%) was obtained as an oily compound by column chromatography (6–25% acetone in dichloromethane) with the LC-MS purity of 99%. [α]$_D$ −11.6 (c 0.3, CHCl$_3$). ^{1}H NMR (400 MHz, CDCl$_3$): 0.58 (s, 3H, H-18), 1.01 (s, 3H, H-19), 1.85 (s, 3H, H-21), 1.93–1.98 (m, 2H, HOOC–CH$_2$–CH$_2$–CH$_2$), 2.37 (t, J = 7.3 Hz, 2H, HOOC–CH$_2$–CH$_2$–CH$_2$), 2.42 (t, J = 7.3 Hz, 2H, HOOC–CH$_2$–CH$_2$–CH$_2$), 4.55–4.68 (m, 1H, H-3), 5.08 (s, 2H, N–O–CH$_2$-), 5.37 (dd, J = 4.5, 2.8 Hz, 1H, H-6), 7.28–7.37 (m, 5H, phenyl). ^{13}C NMR (101 MHz, CDCl$_3$): δ 178.16 (COOH), 172.47 (ester CO), 158.11 (C=N–O), 139.76 (C-5), 138.83 (arom), 128.37 (arom), 128.30 (arom), 128.21 (arom), 128.09 (arom), 127.55 (arom), 122.63 (C-6), 75.44 (N–O–CH$_2$), 74.15 (C-3), 56.86, 56.29, 50.19, 43.80, 38.75, 38.23, 37.11, 36.75, 33.69, 33.03, 32.14, 31.91, 27.89, 24.38, 23.21, 21.12, 20.09, 19.46, 16.19, 13.26. IR spectrum (CHCl$_3$): 3513 (COOH), 3089, 3065, 3030, 1496, 1454, 1185, 1157, 917, 839, 699 (phenyl), 2672 (OH), 1728, 1713 (C=O), 1665 (C=C), 1630 (C=N). MS (ESI): m/z 536.3 (100%, M + H). HR-MS (ESI) m/z: For C$_{33}$H$_{46}$O$_5$N [M + H] calcd, 536.3370; found, 536.3370.

20-Oxo-pregn-5-en-3β-yl hemisuccinate O-ethyloxime (22). Compound **22** was prepared according to general procedure. Starting from compound **27** (208 mg, 0.50 mmol), compound **22** (164 mg, 71%) was obtained as an amorphous compound by column chromatography (10–50% acetone in dichloromethane). Recrystallization from acetone/heptane afforded LC-MS purity of 99%. Mp 151–152 °C. [α]$_D$ −20.2 (c 0.15, CHCl$_3$). ^{1}H NMR (400 MHz, CDCl$_3$): δ 0.64 (s, 3H, H-18), 1.02 (s, 3H, H-19), 1.23 (t, 3H, J = 7.0 Hz, O–CH$_2$–CH$_3$), 1.82 (s, 3H, H-21), 2.60 (t, J = 6.1 Hz, 2H, HOOC–CH$_2$–CH$_2$), 2.65 (t, J = 6.1 Hz, 2H, HOOC–CH$_2$–CH$_2$), 4.04–4.11 (m, 2H, O–CH$_2$–CH$_3$), 4.58–4.68 (m, 1H, H-3), 5.37 (d, J = 5.0 Hz, 1H, H-5). ^{13}C NMR (101 MHz, CDCl$_3$): δ 177.48 (COOH), 171.82 (ester CO), 157.25 (C=N–O), 139.73 (C-5), 122.71 (C-6), 74.61 (C-3), 68.82 (O–CH$_2$–CH$_3$), 56.89, 56.31, 50.22, 43.79, 38.77, 38.15, 37.12, 36.78, 32.16, 31.95, 29.48, 29.22, 27.83, 24.43, 23.30, 21.15, 19.48, 15.94, 14.92, 13.33 (O–CH$_2$–CH$_3$). IR spectrum (CHCl$_3$): 3517, 3100 (COOH), 2672, 2577 (OH), 1728 (ester C=O), 1717 (C=O), 1671 (C=C), 1628 (C=N). MS (negative ESI): m/z 459.3 (26%, M), 458.3 (100%, M − H). HR-MS (negative ESI) m/z: For C$_{27}$H$_{40}$O$_5$N [M − H] calcd, 458.2912; found, 458.2911.

20-Oxo-pregn-5-en-3β-yl hemiadipate O-ethyloxime (23). Compound **23** was prepared according to general procedure. Starting from compound **28** (148 mg, 0.33 mmol), compound **23** (94 mg, 58%) was obtained as an amorphous compound by column chromatography (15–30% acetone in dichloromethane) with an LC-MS purity of 99%. Mp 113–115 °C. [α]$_D$ −21.4 (c 0.17, CHCl$_3$). ^{1}H NMR (400 MHz, CDCl$_3$): δ 0.64 (s, 3H, H-18), 1.02 (s, 3H, H-19), 1.23 (t, J = 7.0 Hz, 3H, O–CH$_2$–CH$_3$), 1.81 (s, 3H, H-21), 1.84–1.87 (m, 2H, HOOC–CH$_2$–CH$_2$–CH$_2$–CH$_2$), 2.28–2.38 (m, 6H, HOOC–CH$_2$–CH$_2$–CH$_2$–CH$_2$), 4.07 (q, J = 7.0 Hz, 2H, O–CH$_2$–CH$_3$), 4.62 (td, J = 8.6, 7.8, 3.3 Hz, 1H, H-3), 5.37 (d, J = 4.9 Hz, 1H, H-5). ^{13}C NMR (101 MHz, CDCl$_3$): δ 178.58 (COOH), 172.87 (ester CO), 157.25 (C=N–O), 139.82 (C-5), 122.62 (C-6), 74.02 (C-3), 68.81 (O–CH$_2$–CH$_3$), 56.89, 56.30, 50.23, 43.78, 38.77, 38.25, 37.15, 36.79, 34.38, 33.68, 32.16, 31.94, 27.92, 24.53, 24.42, 24.24, 23.29, 21.14, 19.48, 15.93, 14.92, 13.33 (O–CH$_2$–CH$_3$). IR spectrum (CHCl$_3$): 3517, 3091 (COOH), 2670, 2565 (OH), 1736 (acid C=O), 1725 (ester C=O), 1713 (C=O), 1670 (C=C). MS (negative ESI): m/z 487.3 (14%, M), 486.3 (100%, M − H). HR-MS (negative ESI) m/z: For C$_{29}$H$_{44}$O$_5$N [M − H] calcd, 486.3225; found, 486.3227.

20-(Ethyloxyimino)-pregn-5-en-3β-ol (24). Compound **24** was prepared according to the general procedure. Starting from pregnenolone (100 mg, 0.32 mmol), compound **24** (112 mg, 98%) was obtained as an amorphous solid compound by column chromatography (10–20% acetone in dichloromethane). Recrystallization from acetone/heptane afforded an LC-MS purity of 99%. Mp 111–113 °C. [α]$_D$ −28.7 (c 0.3, CHCl$_3$). ^{1}H NMR (400 MHz, CDCl$_3$): δ 0.64 (s, 3H, H-18), 1.01 (s, 3H, H-19), 1.23 (t, 3H, J = 7.0 Hz, O–CH$_2$–CH$_3$), 1.82 (s, 3H, H-21), 3.52 (tdd, J = 11.0, 5.2, 4.1 Hz, 1H, H-3), 4.07 (q, J = 7.0 Hz, 2H, O–CH$_2$–CH$_3$), 5.35 (dt, J = 5.3, 2.0 Hz, 1H, H-6). ^{13}C NMR (101 MHz, CDCl$_3$): δ 157.29 (C=N–O), 140.93 (C-5), 121.68 (C-6), 71.89 (C-3), 68.82 (O–CH$_2$–CH$_3$), 56.89, 56.37, 50.33, 43.80, 42.42, 38.81, 37.41, 36.69, 32.20, 31.95, 31.78, 24.44, 23.29,

21.19, 19.57, 15.91, 14.92, 13.34 (O–CH$_2$–CH$_3$). IR spectrum (CHCl$_3$): 3607 (OH), 3009 (=CH), 1667 (C=C), 1620 (C=N). MS (ESI): m/z 360.3 (100%, M + H). HR-MS (ESI) m/z: For C$_{23}$H$_{38}$O$_2$N [M + H] calcd, 360.2897; found, 360.2897.

Alternative synthesis: a stirred solution of pregnenolone (500 mg, 1.5 mmol) in dry pyridine (5 mL) and dry triethylamine (5 mL) was treated with *O*-ethylhydroxylamine hydrochloride (318 mg, 3.15 mmol). The progress of the reaction was repeatedly checked by TLC. After 70 h, the reaction mixture was quenched with water with crushed ice, and a white precipitate was collected, washed with water, and dried. The crude material was purified by column chromatography (10–25% acetone in dichloromethane), affording compound **24** (568 mg, 92%).

20-Oxo-pregn-5-en-3β-yl hemiglutarate (25). Compound **25** was prepared according to the literature[20] with an LC-MS purity of 99%. Mp 139–141 °C, lit.[20] 137–139 °C. [α]$_D$ +9.3 (*c* 0.150, CHCl$_3$), lit.[20] +9.1 (*c* 0.3, CHCl$_3$). ^{1}H NMR (400 MHz, CDCl$_3$): δ 0.62 (s, 3H, H-18), 1.00 (s, 3H, H-19), 1.90–1.98 (m, 2H, HOOC–CH$_2$–CH$_2$–CH$_2$), 2.11 (s, 3H, H-21), 2.36 (t, *J* = 7.3 Hz, 2H, HOOC–CH$_2$–CH$_2$–CH$_2$), 2.42 (t, *J* = 7.3 Hz, 2H, HOOC–CH$_2$–CH$_2$–CH$_2$), 2.52 (1H, t, *J* = 8.9, H-17), 4.53–4.66 (m, 1H, H-3), 5.36 (d, *J* = 5.1, 1H, H-6). ^{13}C NMR (101 MHz, CDCl$_3$): δ 209.88 (C=O), 178.72 (COOH), 172.43 (ester CO), 139.71 (C-5), 122.49 (C-6), 74.09 (C-3), 63.80, 56.95, 50.00, 44.12, 38.90, 38.18, 37.10, 36.72, 33.65, 33.09, 31.93, 31.88, 31.65, 27.86, 24.60, 22.96, 21.15, 20.03, 19.42, 13.33.

17-Oxo-androst-5-en-3β-yl hemiglutarate (26). Compound **26** was prepared according to the literature[20] with an LC-MS purity of 99%. Mp 120–121 °C, lit.[20] 126–128 °C. [α]$_D$ +0.0 (*c* 0.164, CHCl$_3$), lit.[20] +0.0 (*c* 0.2, CHCl$_3$). ^{1}H NMR (400 MHz, CDCl$_3$): δ 0.88 (s, 3H, H-18), 1.04 (s, 3H, H-19), 1.92–1.98 (m, 2H, HOOC–CH$_2$–CH$_2$–CH$_2$), 2.37 (t, *J* = 7.3 Hz, 2H, HOOC–CH$_2$–CH$_2$–CH$_2$), 2.41–2.45 (m, 2H, HOOC–CH$_2$– CH$_2$–CH$_2$), 4.58–4.67 (m, 1H, H-3), 5.40 (1H, d, *J* = 4.0, H-6). ^{13}C NMR (101 MHz, CDCl$_3$): δ ketone at 221 is not visible (the scale of the measurement was below 219.5 PPM), 178.56 (COOH), 172.40 (ester CO), 140.00 (C-5), 122.05 (C-6), 73.99 (C-3), 51.84, 50.27, 47.68, 38.21, 37.05, 36.87, 35.98, 33.65, 33.06, 31.60, 31.54, 30.91, 27.85, 22.02, 20.46, 20.05, 19.48, 13.68.

20-Oxo-pregn-5-en-3β-yl hemisuccinate (27). Compound **27** was prepared according to the literature[20] with an LC-MS purity of 99%. Mp 164–165 °C, lit.[20] 161–163 °C. [α]$_D$ +11.6 (*c* 0.2, CHCl$_3$), lit.[20] +14.3 (*c* 0.2, CHCl$_3$). ^{1}H NMR (400 MHz, CDCl$_3$): δ 0.63 (s, 3H, H-18), 1.02 (s, 3H, H-19), 2.12 (s, 3H, H-21), 2.53 (t, *J* = 8.9, 1H, H-17), 2.60 (ddd, *J* = 7.7, 5.8, 1.5 Hz, 2H, HOOC–CH$_2$–CH$_2$), 2.66–2.70 (m, 2H, HOOC–CH$_2$– CH$_2$–CH$_2$), 4.59–4.68 (m, 1H, H-3), 5.37–5.39 (m, 1H, H-6). ^{13}C NMR (101 MHz, CDCl$_3$): δ 209.81 (C=O), 177.35 (COOH), 171.70 (ester CO), 139.70 (C-5), 122.58 (C-6), 74.55 (C-3), 63.83, 56.99, 50.02, 44.14, 38.93, 38.11, 37.11, 36.74, 31.96, 31.91, 31.69, 29.38, 29.02, 27.80, 24.63, 22.98, 21.18, 19.44, 13.37.

20-Oxo-pregn-5-en-3β-yl hemiadipate (28). Compound **28** was prepared according to the literature[20] with an LC-MS purity of 99%. Mp 135–138 °C, lit.[20] 135–136 °C. [α]$_D$ +10.5 (*c* 0.2, CHCl$_3$), lit.[20] +3.0 (*c* 0.2, CHCl$_3$). ^{1}H NMR (400 MHz, CDCl$_3$): δ 0.60 (s, 3H, H-18), 0.99 (s, 3H, H-19), 1.80–1.87 (m, 2H, H-adipate), 2.09 (s, 3H, H-21), 2.25–2.32 (m, 4H, H-adipate), 2.51 (1H, t, *J* = 8.9,

H-17), 4.53–4.62 (m, 1H, H-3), 5.33–5.36 (m, 1H, H-6). ^{13}C NMR (101 MHz, CDCl$_3$): δ 209.67 (C=O), 176.04 (COOH), 172.90 (ester CO), 139.77 (C-5), 122.36 (C-6), 73.78 (C-3), 63.75, 56.90, 49.95, 44.06, 38.85, 38.15, 37.07, 36.67, 34.39, 33.76, 31.89, 31.83, 31.62, 27.82, 24.57, 24.55, 24.40, 22.89, 21.10, 19.38, 13.29.

Biological assay methods

Transfection and maintenance of the HEK293 cells. HEK293 cells (American Type Culture Collection, ATCC No. CRL-1573, Rockville, MD, USA) were cultured in Opti-MEM I (Invitrogen, Carlsbad, CA, USA) supplemented with 5% fetal bovine serum (FBS; PAN Biotech, Aidenbach, Germany) at 37 °C in 5% CO$_2$. 24 h before transfection, HEK293 cells were plated in 24-well plates at a density of 2 × 10^5 cells per well. The next day, the cells were transfected with cDNA encoding rat GluN1-1a (GluN1; GenBank accession number U08261)[56] and GluN2B (GenBank accession number M91562)[57] subunits (in the pCI-neo expression vector), along with green fluorescent protein (GFP; in the pQBI 25 vector, Takara, Tokyo, Japan). Briefly, equal amounts (200 ng) of cDNAs encoding GluN1-1a, GluN2B, and GFP were mixed with 0.6 µl of Matra-A reagent (IBA, Gottingen, Germany) in 50 µL of Opti-MEM I and added to confluent HEK293 cells cultured in 24-well plates. After trypsinization, the cells were resuspended in Opti-MEM I containing 1% FBS, supplemented with 20 mM MgCl$_2$, 1 mM D,L-2-amino-5-phosphonovaleric acid, 3 mM kynurenic acid, and 1 µM ketamine, and plated on 30 mm glass coverslips coated with collagen and poly-L-lysine. Transfected cells were identified by GFP epifluorescence. Electrophysiology experiments were performed 24–48 h after transfection.

Electrophysiology in HEK293 cells. Whole-cell current recordings, voltage-clamped at a holding potential of −60 mV, were performed at room temperature using a patch-clamp amplifier (Axopatch 200B; Molecular Devices, Sunnyvale, CA, USA) after capacitance and series resistance (<10 MΩ) compensation (80–90%). NMDAR current responses were low-pass filtered at 2 kHz, digitally sampled at 5 kHz, and analysed using pClamp software (version 10.6; Molecular Devices). Patch pipettes (3–5 MΩ), pulled from borosilicate glass, were filled with an intracellular solution (ICS) containing (in mM): 15 CsCl, 10 BAPTA, 3 MgCl$_2$, 1 CaCl$_2$, 120 gluconic acid, 10 HEPES, and 2 ATP-Mg salt (pH adjusted to 7.2 with CsOH). The extracellular solution (ECS) contained (in mM): 160 NaCl, 2.5 KCl, 0.2 EDTA, 10 glucose, 10 HEPES, and 0.7 CaCl$_2$ (pH adjusted to 7.3 with NaOH). NMDAR responses were induced by 1 µM glutamate and 30 µM glycine. 1% DMSO was present in all control and testing solutions. Solution applications were performed using a microprocessor-controlled multibarrel fast-perfusion system with a solution exchange rate around the cells of ~10 ms.[58]

In vitro ADME profiling

Microsomal stability. Microsomal stability assay was performed using the 1 mg mL^{-1} rat pooled liver microsomal preparation (Thermo Scientific) and 10 µM compounds in 90 mM TRIS-Cl buffer pH 7.4 containing 2 mM NADPH and

2 mM MgCl2 for 0, 30, and 60 min at 37 °C. Reference compound Verapamil was also tested to provide positive control data for this assay. The reactions were terminated by the addition of four volumes of ice-cold methanol, mixed vigorously, and left at −20 °C for 1h. After that, the samples were centrifuged and the supernatants were analysed by means of ECHO-MS® System (Sciex, Framingham, MA, USA). Zero time points were prepared by adding ice-cold methanol to the mixture of the compound with cofactors before the addition of microsomes. The microsomal half-lives ($t_{1/2}$) were calculated using the equation $t_{1/2} = 0.693/k$, where k is the slope found in the linear fit of the natural logarithm for the fraction remaining of the parent compound *vs.* incubation time. Intrinsic clearance (CL_{int}) was calculated using the following formula:

$$CL_{int} = V \times \frac{\ln 2}{t_{1/2}}$$

where V is the incubation volume per milligram of microsomal protein ($\mu L\ mg^{-1}$) and $t_{1/2}$ is the microsomal half-life.

PAMPA permeability. Permeation experiments were conducted in polystyrene 96-well filter plates with PVDF membrane pre-coated with structured layers of phospholipids (Corning Gentest™) according to the manufacturer's instructions. Briefly, the plate was warmed to room temperature, and meanwhile, the solutions of the compounds were diluted from 10 mM DMSO stocks to TRIS–HCl buffer pH 7.4 to reach a 100 μM final concentration. The DMSO concentration in the samples was 1%. Then, 300 μL of these solutions were transferred into the donor (receiver) plate wells, and 200 μL of the (TRIS) buffer was added to the acceptor (filter) plate wells. The filter plate and receiver plate were assembled and incubated for 5 h on an orbital shaker (300 rpm). After this, the concentration of the tested substances in both the donor and acceptor compartments was determined with use of LC/MS. Liquid chromatography was performed using an ExionLC AD pump and autosampler from Sciex (Framingham, MA, USA). The mobile phase was (A) 0.1% formic acid in water and (B) 0.1% formic acid in acetonitrile with the following gradient: 0–1 min 2% (B); 1–5 min 2–98% (B); 5–6 min 98% (B); 6–8 min 2% (B). The mobile phase flow rate was 300 $\mu L\ min^{-1}$. The column Synergi Fusion-RP from Phenomenex (Torrance, CA, USA) was used and was kept at 40 °C during the analysis. Actual compound concentration in the samples was quantified by means of multiple reaction monitoring (MRM) mass spectrometry using the Sciex QTRAP® 6500+. Permeability coefficients P_e ($cm\ s^{-1}$) and mass retention R (%) were calculated using the following formulas:

$$P_e = -\frac{\ln\left[1 - \dfrac{C_A(t)}{C_{equilibrium}}\right]}{A \times \left(\dfrac{1}{V_D} + \dfrac{1}{V_A}\right) \times t}$$

$$R = 100 \times (1 - [C_D(t) \times V_D + C_A(t) \times V_A]/(C_0 \times V_D))$$

where C_0 is the initial compound concentration in donor well (mM), $C_D(t)$ is the compound concentration in donor well at time t (mM), $C_A(t)$ is the compound concentration in acceptor well at time t (mM), V_D is the donor well volume (0.3 mL), V_A is the acceptor well volume (0.2 mL), $C_{equilibrium} = C_D(t) \times V_D + C_A(t) \times V_A/(V_D + V_A)$, A is the filter area (0.3 cm^2) and t is the incubation time (18 000s = 5 h).

Stability in rat hepatocytes. Primary rat hepatocytes were isolated from 12-weeks-old male Wistar rats ($n = 3$) by two-step collagenase liver perfusion. Tribromoethanol was used as an anesthetic agent at a dose of 250 mg kg^{-1}. Briefly, rat liver was first perfused for 3 min with a pre-perfusing solution (HBSS w/o Ca^{2+} and Mg^{2+}, 20 mM HEPES pH 7.4, 0.5 mM EDTA), then for 3 min with washing solution (HBSS, 20 mM HEPES pH 7.4), and then for 15 min with perfusing solution (HBSS, 20 mM HEPES pH 7.4, 5 mM CaCl$_2$, 5 mM MgCl$_2$, 0.016 mg mL^{-1} collagenase Type II). Flow rate was maintained at 7 mL min^{-1}, and all solutions were kept at 37 °C. After *in situ* perfusion, the liver was excised, the liver capsule was opened, and cells were suspended in William's Medium E and filtered through a 70 μm membrane. Dead cells were removed by Percoll centrifugation (Percoll density: 1.06 g mL^{-1}, 50×g, 10 min, 20 °C) and additional centrifugation in William's Medium E (50×g, 5 min). Cells were subsequently diluted in William's Medium E, and their viability and cell suspension density were determined by Trypan Blue exclusion using a hemocytometer. Then, 10 mM DMSO stock solution of each test compound was diluted to 6 μM (2× concentration; final DMSO concentration – 0.25%) using William's Medium E to create the working samples. Aliquots (50 μL) of the hepatocyte suspension were added to each test well of a 96-well plate, immediately followed by the addition of a 50 μL aliquot of the test compound or control solutions (final hepatocyte density – 0.5 × 10^6 mL^{-1}). The samples for each time point (0, 5, 10, 20, 40, 60, and 120 min) were prepared in duplicates for all the test and reference compounds. Incubations were done at 37 °C, 5% CO$_2$, and 95% relative humidity in a CO$_2$ incubator. At appropriate time-points, 40 μL aliquots were removed from the wells and placed in 1.1 mL microtubes containing 200 μL of methanol and used for LC-MS/MS analysis.

Elimination constant (k_{el}), half-life ($t_{1/2}$), and intrinsic clearance (CL_{int}) were determined in plots of ln (percent remaining of parent compound) *versus* time, using linear regression analysis:

$$k = -slope$$

$$t_{1/2} = \frac{\ln 2}{-k}$$

$$Cl_{int} = \frac{\ln 2}{t_{1/2}}$$

$$\times \frac{\text{Incubation volume } (\mu L)}{\text{Number of cells in incubation } (10^6)} \,(\mu L \text{ per min per } 10^6 \text{cells})$$

Stability in rat plasma. Compounds were prepared as 1.6 mg mL^{-1} stock solutions in methanol. Then, 20 μL of stock solution was added to 1000 μL of rat plasma (BioIVT, Cat. No. RAT00PLLH-0102307), maintained at 37 °C. Aliquots (50 μL) withdrawn at 0, 8, and 24 h were analyzed by HPLC. An aliquot of plasma was extracted with methanol (450 μL) containing an internal standard, and the solution was vortexed (20 s) and centrifuged at 13 500 rpm for 10 min. The supernatant was transferred to an autosampler vial, and 10 μL was injected into an LC-MS system. The samples were analyzed using an Agilent 6230 TOF LC/MS. Samples were separated on a Waters ACQUITY UPLC CSH Phenyl-Hexyl column (100 × 2.1, 130 Å, 1.7 μm) at a flow rate of 0.3 mL min^{-1}. The concentration of mobile phase B (0.1% formic acid in acetonitrile) was gradually increased from 10 to 100% in mobile phase A (0.1% formic acid in water) over 7 min. The mass spectrometry instrument was operated in a negative ion mode with a voltage of +3.00 kV applied to the capillary. The temperature, the flow rate of the nitrogen drying gas, the pressure of the nitrogen nebulizing gas, and the flow rate of the sheath gas were set at 325 °C, 10 L min^{-1}, 40 psi, 390 °C, and 11 L min^{-1}, respectively. Results are represented as a percentage of the compound remaining in spiked plasma.

Thermodynamic solubility. The reference samples were prepared as follows: a weight corresponding to 2.5 μmol was dissolved in 250 μL of DMSO, resulting in a concentration of 10 mM stock solution. Each calibration level standard was prepared by diluting the stock solution in a mixture of PBS and acetonitrile (50 : 50 v/v). The samples for testing were prepared as follows: the volume of 1000 μL of PBS was added to the testing tube containing a weight of sample corresponding to 0.4 mM. The mixture was shaken at 1000 rpm at 20 °C for 24 h. The mixture was then filtered using a syringe polypropylene 0.45 μm filter. Samples and calibration standards are prepared using an automated system of a robotic arm (PAL-RTC, Switzerland). Then, the sample was analysed on chromatographic system (Vanquish UHPLC, Thermo Fisher Scientific, Germany) connected to the diode array detector and consequently to the charged aerosol detector (both Vanquish, Thermo Fisher Scientific, Germany), Thermo Scientific Accucore C8 (100 × 3 mm; 2.6 μm) column, using gradient elution with acetonitrile/methanol/5 mM formate buffer (pH = 3.00); flow: 1.0 cm^3 min^{-1}; column temperature: 40 °C; CAD temperature: 30 °C; sample volume: 5 mm^3.

Conclusions

A series of novel C-17 and C-20 steroidal oximes and oxime ethers were designed, synthesized, and evaluated as PAMs of GluN1/GluN2B NMDA receptors using the patch-clamp technique. SAR analysis demonstrated that oxime ether modification at the C-20 position significantly influenced both efficacy and potency, with several compounds being more potent or efficacious than the endogenous reference compound, pregnenolone sulfate (**PES**). Notably, compounds **12** and **17** exhibited the highest efficacy (E_{max} = 673% and 503%, respectively) and potent activity in the low micromolar range (EC$_{50}$ = 8.7 μM and 6.1 μM, respectively).

Pregnenolone derivatives within this study consistently provided superior PAM activity compared to their DHEA analogues. Certain derivatives (*e.g.*, compounds **18** and **19**) displayed concentration-dependent biphasic modulation, suggesting complex interaction with the NMDAR. Additionally, extension of the C-3 hemiester moiety (compounds **22** and **23**) did not yield further improvement in PAM mode over compound **12**.

In vitro ADME profiling confirmed that the oxime ether scaffold affords favourable drug-like properties, including excellent metabolic and plasma stability, and enhanced solubility. Compound **12** was identified as the lead candidate based on its balanced profile of pharmacological activity and physicochemical properties for further optimization for central nervous system-targeted therapeutic development.

Collectively, the SAR trends underscore that minimal, conformationally flexible C-20 oxime ethers on a planar pregnenolone 5-ene scaffold, combined with a C-3 hemiester, provide an optimal balance of receptor engagement, aqueous solubility, and metabolic stability, which explains their superior PAM activity relative to PES and earlier 20-keto analogues.

Author contributions

Conflicts of interest

There are no conflicts to declare.

Ethical statement

This study utilized commercially sourced plasma purchased from BioIVT, Cat. No. RAT00PLLH-0102307 (rat). Because all biological material was obtained as certified reagent from a commercial provider, this research did not involve animal subjects. All procedures were conducted in accordance with laboratory biosafety guidelines (BSL-2) for handling animal-derived materials.

Data availability

The data supporting this article have been included as part of the supplementary information (SI). Supplementary information is available. See DOI: https://doi.org/10.1039/d5ra07716h.

Acknowledgements

References

1 E. Kudova, *Neurosci. Lett.*, 2021, **750**, 135771.

2 M. Korinek, V. Kapras, V. Vyklicky, E. Adamusova, J. Borovska, K. Vales, A. Stuchlik, M. Horak, H. Chodounska and L. Vyklicky Jr, *Steroids*, 2011, **76**, 1409–1418.

3 K. B. Hansen, L. P. Wollmuth, D. Bowie, H. Furukawa, F. S. Menniti, A. I. Sobolevsky, G. T. Swanson, S. A. Swanger, I. H. Greger, T. Nakagawa, C. J. McBain, V. Jayaraman, C. M. Low, M. L. Dell'Acqua, J. S. Diamond, C. R. Camp, R. E. Perszyk, H. Yuan and S. F. Traynelis, *Pharmacol. Rev.*, 2021, **73**, 298–487.

4 S. Gataullina, T. Bienvenu, R. Nabbout, G. Huberfeld and O. Dulac, *Dev. Med. Child Neurol.*, 2019, **61**, 891–898.

5 R. Celli and F. Fornai, *Curr. Neuropharmacol.*, 2021, **19**, 747–765.

6 G. D. Mangano, A. Riva, A. Fontana, V. Salpietro, G. R. Mangano, G. Nobile, A. Orsini, M. Iacomino, R. Battini, G. Astrea, P. Striano and R. Nardello, *Epilepsy Behav.*, 2022, **129**, 108604.

7 W. A. Jumaili, C. Trivedi, T. Chao, A. Kubosumi and S. Jain, *Behav. Brain Res.*, 2022, **424**, 113804.

8 I. D. Henter, L. T. Park and C. A. Zarate Jr, *CNS Drugs*, 2021, **35**, 527–543.

9 S. Obeng, T. Hiranita, F. Leon, L. R. McMahon and C. R. McCurdy, *J. Med. Chem.*, 2021, **64**, 6523–6548.

10 Y. Meng and H. L. Shen, *J. Pain Res.*, 2022, **15**, 2005–2013.

11 Z. Shen, M. Xiang, C. Chen, F. Ding, Y. Wang, C. Shang, L. Xin, Y. Zhang and X. Cui, *Biomed. Pharmacother.*, 2022, **151**, 113125.

12 G. E. Hardingham and H. Bading, *Nat. Rev. Neurosci.*, 2010, **11**, 682–696.

13 C. Hu, W. Chen, S. J. Myers, H. Yuan and S. F. Traynelis, *J. Pharmacol. Sci.*, 2016, **132**, 115–121.

14 J. Tarabeux, O. Kebir, J. Gauthier, F. F. Hamdan, L. Xiong, A. Piton, D. Spiegelman, E. Henrion, B. Millet, S. D. team, F. Fathalli, R. Joober, J. L. Rapoport, L. E. DeLisi, E. Fombonne, L. Mottron, N. Forget-Dubois, M. Boivin, J. L. Michaud, P. Drapeau, R. G. Lafreniere, G. A. Rouleau and M. O. Krebs, *Transl. Psychiatry*, 2011, **1**, e55.

15 W. Tang, D. Liu, S. F. Traynelis and H. Yuan, *Neuropharmacology*, 2020, **177**, 108247.

16 F. F. Hamdan, J. Gauthier, Y. Araki, D. T. Lin, Y. Yoshizawa, K. Higashi, A. R. Park, D. Spiegelman, S. Dobrzeniecka, A. Piton, H. Tomitori, H. Daoud, C. Massicotte, E. Henrion, O. Diallo, S. D. Group, M. Shekarabi, C. Marineau, M. Shevell, B. Maranda, G. Mitchell, A. Nadeau, G. D'Anjou, M. Vanasse, M. Srour, R. G. Lafreniere, P. Drapeau, J. C. Lacaille, E. Kim, J. R. Lee, K. Igarashi, R. L. Huganir, G. A. Rouleau and J. L. Michaud, *Am. J. Hum. Genet.*, 2011, **88**, 306–316.

17 L. Fedele, J. Newcombe, M. Topf, A. Gibb, R. J. Harvey and T. G. Smart, *Nat. Commun.*, 2018, **9**, 957.

18 M. Elmasri, J. S. Lotti, W. Aziz, O. G. Steele, E. Karachaliou, K. Sakimura, K. B. Hansen and A. C. Penn, *Brain Sci.*, 2022, **12**(6), 789.

19 E. Kudova, H. Chodounska, B. Slavikova, M. Budesinsky, M. Nekardova, V. Vyklicky, B. Krausova, P. Svehla and L. Vyklicky, *J. Med. Chem.*, 2015, **58**, 5950–5966.

20 B. Krausova, B. Slavikova, M. Nekardova, P. Hubalkova, V. Vyklicky, H. Chodounska, L. Vyklicky and E. Kudova, *J. Med. Chem.*, 2018, **61**, 4505–4516.

21 B. Slavikova, H. Chodounska, M. Nekardova, V. Vyklicky, M. Ladislav, P. Hubalkova, B. Krausova, L. Vyklicky and E. Kudova, *J. Med. Chem.*, 2016, **59**, 4724–4739.

22 S. K. Adla, B. Slavikova, M. Smidkova, E. Tloustova, M. Svoboda, V. Vyklicky, B. Krausova, P. Hubalkova, M. Nekardova, K. Holubova, K. Vales, M. Budesinsky, L. Vyklicky, H. Chodounska and E. Kudova, *Steroids*, 2017, **117**, 52–61.

23 S. K. Adla, B. Slavikova, H. Chodounska, V. Vyklicky, M. Ladislav, P. Hubalkova, B. Krausova, T. Smejkalova, M. Nekardova, M. Smidkova, L. Monincova, R. Soucek, L. Vyklicky and E. Kudova, *Front. Pharmacol*, 2018, **9**, 1299.

24 M. Smidkova, M. Hajek, S. K. Adla, B. Slavikova, H. Chodounska, M. Matousova, H. Mertlikova-Kaiserova and E. Kudova, *J. Steroid Biochem. Mol. Biol.*, 2019, **189**, 195–203.

25 C. E. Weaver, M. B. Land, R. H. Purdy, K. G. Richards, T. T. Gibbs and D. H. Farb, *J. Pharmacol. Exp. Ther.*, 2000, **293**, 747–754.

26 J. Borovska, V. Vyklicky, E. Stastna, V. Kapras, B. Slavikova, M. Horak, H. Chodounska and L. Vyklicky Jr, *Br. J. Pharmacol.*, 2012, **166**, 1069–1083.

27 N. Yaghoubi, A. Malayev, S. J. Russek, T. T. Gibbs and D. H. Farb, *Brain Res.*, 1998, **803**, 153–160.

28 G. A. Patani and E. J. LaVoie, *Chem. Rev.*, 1996, **96**, 3147–3176.

29 N. A. Meanwell, *J. Med. Chem.*, 2011, **54**, 2529–2591.

30 B. Macchia, A. Balsamo, A. Lapucci, A. Martinelli, F. Macchia, M. C. Breschi, B. Fantoni and E. Martinotti, *J. Med. Chem.*, 1985, **28**, 153–160.

31 J. Dhuguru, E. Zviagin and R. Skouta, *Pharmaceuticals*, 2022, **15**(1), 66.

32 D. E. Lorke, H. Kalasz, G. A. Petroianu and K. Tekes, *Curr. Med. Chem.*, 2008, **15**, 743–753.

33 M. N. Faiz Norrrahim, M. A. Idayu Abdul Razak, N. A. Ahmad Shah, H. Kasim, W. Y. Wan Yusoff, N. A. Halim, S. A. Mohd Nor, S. H. Jamal, K. K. Ong, W. M. Zin Wan Yunus, V. F. Knight and N. A. Mohd Kasim, *RSC Adv.*, 2020, **10**, 4465–4489.

34 M. Johansson, M. Mansson, L. E. Lins, B. Scharschmidt, M. Doverskog and T. Backstrom, *Psychopharmacology*, 2018, **235**, 1533–1543.

35 S. Montagnese, M. Lauridsen, H. Vilstrup, L. Zarantonello, G. Lakner, S. Fitilev, I. Zupanets, I. Kozlova, E. Bunkova, K. Tomasiewicz, J. E. Berglund, F. Rorsman, H. Hagstrom, S. Kechagias, C. E. Ocklind, J. Mauney, F. Thunarf, M. Mokhatarani, T. Backstrom, M. Doverskog, L. E. Lins, M. Mansson, P. Samuelson, D. Nilsson, M. Schalling, M. Johansson, E. Arlander and B. F. Scharschmidt, *J. Hepatol.*, 2021, **75**, 98–107.

36 G. Mincheva, C. Gimenez-Garzo, P. Izquierdo-Altarejos, M. Martinez-Garcia, M. Doverskog, T. P. Blackburn, A. Hallgren, T. Backstrom, M. Llansola and V. Felipo, *CNS Neurosci. Ther.*, 2022, **28**, 1861–1874.

37 N. Deive, J. Rodriguez and C. Jimenez, *J. Med. Chem.*, 2001, **44**, 2612–2618.

38 A. Carrasco-Carballo, M. Guadalupe Hernandez-Linares, M. Cardenas-Garcia and J. Sandoval-Ramirez, *Steroids*, 2021, **166**, 108787.

39 P. C. Acharya and R. Bansal, *Arch. Pharm.*, 2014, **347**, 193–199.

40 L. Nahar, S. D. Sarker and A. B. Turner, *Chem. Nat. Compd.*, 2008, **44**, 315–318.

41 M. I. Sikharulidze, N. S. Nadaraia, M. L. Kakhabrishvili, N. N. Barbakadze and K. G. Mulkidzhanyan, *Chem. Nat. Compd.*, 2010, **46**, 493–494.

42 D. B. Guthrie, D. G. Stein, D. C. Liotta, M. A. Lockwood, I. Sayeed, F. Atif, R. F. Arrendale, G. P. Reddy, T. J. Evers, J. R. Marengo, R. B. Howard, D. G. Culver and M. G. Natchus, *ACS Med. Chem. Lett.*, 2012, **3**, 362–366.

43 M. K. Christensen, K. D. Erichsen, U. H. Olesen, J. Tjornelund, P. Fristrup, A. Thougaard, S. J. Nielsen, M. Sehested, P. B. Jensen, E. Loza, I. Kalvinsh, A. Garten, W. Kiess and F. Bjorkling, *J. Med. Chem.*, 2013, **56**, 9071–9088.

44 M. Horak, K. Vlcek, M. Petrovic, H. Chodounska and L. Vyklicky Jr, *J. Neurosci.*, 2004, **24**, 10318–10325.

45 B. Kysilov, B. Hrcka Krausova, V. Vyklicky, T. Smejkalova, M. Korinek, M. Horak, H. Chodounska, E. Kudova, J. Cerny and L. Vyklicky, *Br. J. Pharmacol.*, 2022, **179**, 3970–3990.

46 H. Zemkova, V. Tvrdonova, A. Bhattacharya and M. Jindrichova, *Physiol. Res.*, 2014, **63**(1), S215–S224.

47 J. Bukanova, E. Solntseva, R. Kondratenko and E. Kudova, *Biomolecules*, 2021, 11.

48 E. I. Solntseva, J. V. Bukanova, V. G. Skrebitsky and E. Kudova, *Hippocampus*, 2022, **32**, 552–563.

49 F. Follath, H. R. Ha, E. Schutz and F. Buhler, *Br. J. Clin. Pharmacol.*, 1986, **21**(2), 149S–153S.

50 M. Kansy, A. Avdeef and H. Fischer, *Drug Discov. Today Technol.*, 2004, **1**, 349–355.

51 A. Avdeef, S. Bendels, L. Di, B. Faller, M. Kansy, K. Sugano and Y. Yamauchi, *J. Pharm. Sci.*, 2007, **96**, 2893–2909.

52 S. Carrara, V. Reali, P. Misiano, G. Dondio and C. Bigogno, *Int. J. Pharm.*, 2007, **345**, 125–133.

53 Y. Morofuji and S. Nakagawa, *Curr. Pharm. Des.*, 2020, **26**, 1466–1485.

54 Z. S. Teksin, P. R. Seo and J. E. Polli, *AAPS J.*, 2010, **12**, 238–241.

55 C. Schottler and K. Krisch, *Biochem. Pharmacol.*, 1974, **23**, 2867–2875.

56 M. Hollmann, J. Boulter, C. Maron, L. Beasley, J. Sullivan, G. Pecht and S. Heinemann, *Neuron*, 1993, **10**, 943–954.

57 H. Monyer, R. Sprengel, R. Schoepfer, A. Herb, M. Higuchi, H. Lomeli, N. Burnashev, B. Sakmann and P. H. Seeburg, *Science*, 1992, **256**, 1217–1221.

58 V. Vyklicky, M. Korinek, A. Balik, T. Smejkalova, B. Krausova and L. Vyklicky, in *Ionotropic Glutamate Receptor Technologies*, ed. G. K. Popescu, Springer New York, New York, NY, 2016, pp. 205–219, DOI: 10.1007/978-1-4939-2812-5_14.